Small-Bandgap Conducting Polymers Based on Conjugated Poly(heteroarylene methines). 2. Synthesis, Structure, and Properties

Wen-Chang Chen and Samson A. Jenekhe*

Department of Chemical Engineering and Center for Photoinduced Charge Transfer, University of Rochester, Rochester, New York 14627-0166

Received October 17, 1994®

ABSTRACT: A series of soluble conjugated poly(heteroarylene methines) with varying number of 2,5-thienylene rings have been synthesized, characterized, and shown to have small *intrinsic* optical and electrochemical bandgaps. The conjugated polymers containing alternating aromatic and quinoid heteroarylene moieties in the main chain were prepared by oxidative dehydrogenation of precursor poly(heteroarylene methylenes) with 2,3-dicyano-5,6-dichloro-1,4-benzoquinone (DDQ). The optical and electrochemical properties of the conjugated poly(heteroarylene methines), such as bandgap, redox potentials, ionization potential, and electron affinity, were found to be significantly modified by the size of the quinoid moieties in the main chain and the type of donor or acceptor side group at the methine carbon. Some of the poly(heteroarylene methines) have intrinsic bandgaps (E_g) that are significantly smaller than found for the parent polythiophene ($E_g \sim 2$ eV): PBTHBQ ($E_g = 1.14$ eV); PBTBQ ($E_g = 1.27$ eV); PBTTBQ ($E_g = 1.31$ eV); and PBTNBQ ($E_g = 1.45$ eV). These same four polymers have peak oxidation potentials in the range 0.29–0.54 V (SCE) and peak reduction potentials in the range −1.82 to −1.49 V (SCE). The electrical conductivity of iodine-doped thin films of PBTBQ, PBTNBQ, and PBTHBQ was 6×10^{-3}, 2.2×10^{-3}, and 1.6×10^{-1} S/cm, respectively, compared to a conductivity of less than 10^{-7} S/cm for the undoped materials. These results confirm that conjugated poly(heteroarylene methines) are small-bandgap conducting polymers which can be prepared by oxidative dehydrogenation of precursors.

Introduction

Currently known conducting polymers are prepared from π-conjugated polymers by a chemical or electrochemical process called *doping* which enhances the electrical conductivity of the pristine conjugated polymer by many orders of magnitude from the semiconducting to the metallic range (10^{-7} to 10^{6} S/cm).[1] For example, the well-known conjugated polymer polyacetylene has only a marginal *intrinsic* conductivity of about 10^{-9} S/cm or less in its pristine state whereas when chemically doped, its conductivity is raised to values as high as 10^{5} S/cm.[2] The process of doping increases the conductivity of π-conjugated polymers primarily by the dramatic increase of *extrinsic* charge carrier concentration. Doping is also the source of the well-known chemical instability of conducting polymers. The possible elimination of doping in preparing conducting polymers while still achieving high conductivity was one of the original motivations of experimental work on small-bandgap (E_g) or metallic conducting polymers.[3] However, it was also thought that control of the E_g value of a polymer by molecular design would allow the control of its optical, electronic, and optoelectronic properties.[3] Although there have been a number of theoretical[4–17] and experimental[3,18–28] approaches to achieving small-bandgap conducting polymers, we will focus on the polyheteroarylenes and their derivatives.

In early theoretical studies by Bredas and co-workers, it was shown that the bandgap of polyheteroarylenes, such as polythiophene, was a strong function of molecular geometry.[5] They showed that whereas polythiophene with *aromatic* geometry had a calculated bandgap of about 2 eV, which is close to the experimental value, the similarly calculated E_g value for the *quinoid isomer* was only 0.47 eV:

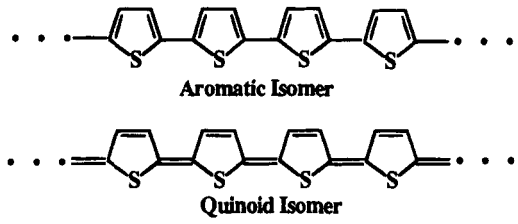

More recent theoretical calculations have confirmed the very small bandgap of quinoid polythiophene, with E_g values as small as 0.26 eV.[6] To test this idea that quinoid geometry can substantially reduce the bandgap of conjugated polyheteroarylenes, Wudl and co-workers synthesized polyisothianaphthene (PITN) and showed

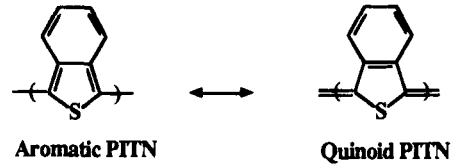

that it has a very small bandgap ($E_g = 1.13$ eV) due to the preferred stabilization of the quinoid resonance form by the fused benzene ring.[19a] The electrochemically synthesized PITN, with an optical bandgap of 1.13 eV, has a lowest energy λ_{max} of 830 nm (1.49 eV) and a conductivity of up to 50 S/cm in the doped state. Theoretical calculations of the E_g values of the two PITN isomers show that the quinoid form ($E_g = 1.16$ eV) is more stable than the aromatic isomer ($E_g = 0.73$ eV).[9a] However, a recent experimental study of electrochemically synthesized PITN suggests that the polymer has

* To whom correspondence should be addressed.

® Abstract published in *Advance ACS Abstracts,* December 15, 1994.

0024-9297/95/2228-0465$09.00/0

a larger $\pi-\pi^*$ transition with λ_{max} = 633 nm (2.0 eV) than previously thought.[20] These authors also suggest that the lowest energy absorption band at 830 nm (1.49 eV) reported by Wudl and co-workers is actually due to a stable bipolaron rather than a $\pi-\pi^*$ transition of the intrinsic neutral PITN. Recent band structure calculations of PITN found a λ_{max} of 2.28 and 0.8 eV for the quinoid and aromatic isomers, respectively.[7] Thus, the true value of the intrinsic bandgap of PITN is now unclear.

One of us[3a] in 1986 first proposed poly(heteroarylene methines) which directly incorporate quinoid moieties in the conjugated polymer backbone as a class of small-bandgap conducting polymers:

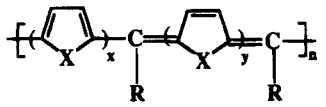

It was thought that by incorporating both aromatic and quinoid isomers in the same polymer chain, materials with bandgap values intermediate between the then known theoretical limits of 0.47 and 2 eV for the quinoid and aromatic geometries would be obtained as the *block sizes x* and *y* were varied.[3a] A general two-step synthetic scheme involving precursor nonconjugated poly(heteroarylene methylenes) that can be subsequently oxidatively dehydrogenated to give the poly(heteroarylene methines) was also proposed.[3] Three members of this class of conjugated polymers initially prepared by such a two-step approach, including oxidative dehydrogenation of the precursor polymers with bromine, had very small bandgaps in the range of 0.75–1.10 eV. However, the polymers resulting from bromine dehydrogenation have been suggested to be partially brominated and partially doped with bromine.[21] Theoretical calculations of the electronic structure of the poly(heteroarylene methines) show that they exhibit small bandgaps ranging from 0.75 to 1.21 eV.[8-10,23f] Boudreaux et al. reported a band structure calculation for poly(*p*-phenylene methines) which indicated a bandgap of 1.17 eV and an ionization potential of 4.2 eV.[8b] They also predicted that a soliton defect could exist in the doped form of this polymer. Kertesz and co-workers[9a,b] have obtained calculated bandgaps of 1.05–1.21 and 0.99 eV for poly(thienylene methines) and poly(pyrrolene methine), respectively. They showed that the small bandgaps of the poly(heteroarylene methines) were due to small bond length alternation values (0.077–0.089 Å) compared to *trans*-polyacetylene (0.102 Å). Bredas and co-workers have also calculated small bandgaps, which are in the range of 0.75–1.10 eV,[10,23f] for poly(pyrrolene methines).

Several synthetic approaches[22-24] to the conjugated poly(heteroarylene methines) and poly(arylene methines) have been reported in addition to the previously mentioned precursor polymer route proposed by one of us.[3a] Fernandez and co-workers have used a Wittig reaction to prepare poly(*p*-phenylene methine).[22c] However, the product was proven to be *p*-distyrylbenzene due to a side reaction.[23a] Braunling and co-workers[23b] used a one-step polycondensation reaction of 2-(chloromethyl)-5-formylfuran with furan or pyrrole to prepare methine-bridged heterocyclic conjugated polymers. The highest conductivity of the resulting polymers doped with I_2 was 10^{-4} S/cm. However, the CP-MAS ^{13}C-NMR spectra of the polymers showed a considerable amount of sp^3 carbon and even some carbonyl carbon.

Chart 1

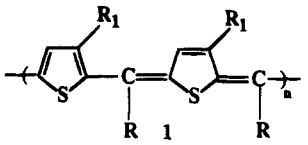

1a. R_1 = H, R =  (PTBQ)

1b. R_1 = H, R = 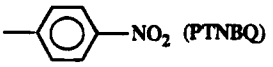 (PTNBQ)

1c. R_1 = CH_3, R =  (PMTBQ)

1d. R_1 = CH_3, R = 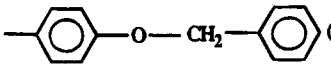 (PMTBBQ)

1e. R_1 = CH_3, R = 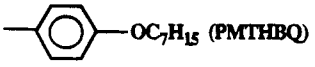 (PMTHBQ)

Hanack et al.[24a] prepared a new poly(arylene methine) containing alternating phenylene and dihydroanthracene units by a one-step polycondensation reaction. However, very low molecular weight and very low conductivity were reported for the product. Becker et al.[23] later reported the preparation of poly(pyrrolyl methine) from the condensation reaction of 2-pyrrolecarbaldehyde with $POCl_3$. The resulting polymer was found to be doped and to contain various impurities such as $POCl_3$ or HCl which could not be removed. Since their previous preparation of poly(arylene methines)[23a-d] led to doped or impure polymers, Braunling et al.[23e,f] looked for very reactive starting compounds that would not need very aggressive reagents for polymerization. They prepared poly(diheteroarylene methines) by polycondensation of heterocyclic dicarbinols. The resulting polymers were prepared as electrically conducting composites with poly(vinyl chloride) and had conductivities of up to 10^{-2} S/cm. Although this synthetic scheme yielded a product which seemed to have the expected poly(thienylene methine) structure, the product did not have a small bandgap as expected. They attributed this inconsistency to the relatively low molecular weight, branched polymer chains and the interruption of the conjugation by readdition of the OH group to the polymer backbone. Recently, Hanack and co-workers have prepared a series of monomers containing quinoid heterocyclic segments such as thiophene, pyrrole, or isothianaphthene.[24b-d] These monomers have a high planarity and good π-electron delocalization (λ_{max} = 390–470 nm) and were proposed to be polymerizable using various coupling reactions. However, the details of the synthesis and characterization of the polymers from such monomers have not yet been reported.

This paper reports the synthesis and detailed characterization of a series of soluble conjugated poly(heteroarylene methines) containing different heteroarylene block size (Charts 1 and 2). The polymers were prepared by the two-step synthetic scheme proposed by one of us.[3] However, the oxidative dehydrogenation of precursor poly(heteroarylene methylenes) was done in solution using 2,3-dicyano-5,6-dichloro-1,4-benzoquinone (DDQ), which has been widely used for the conversion of hydrocarbons, cyclic ketones, and heterocyclic compounds into their unsaturated derivatives.[29,30] The incorporation of bulky side groups R in the conjugated poly(heteroarylene methines) made them

Chart 2

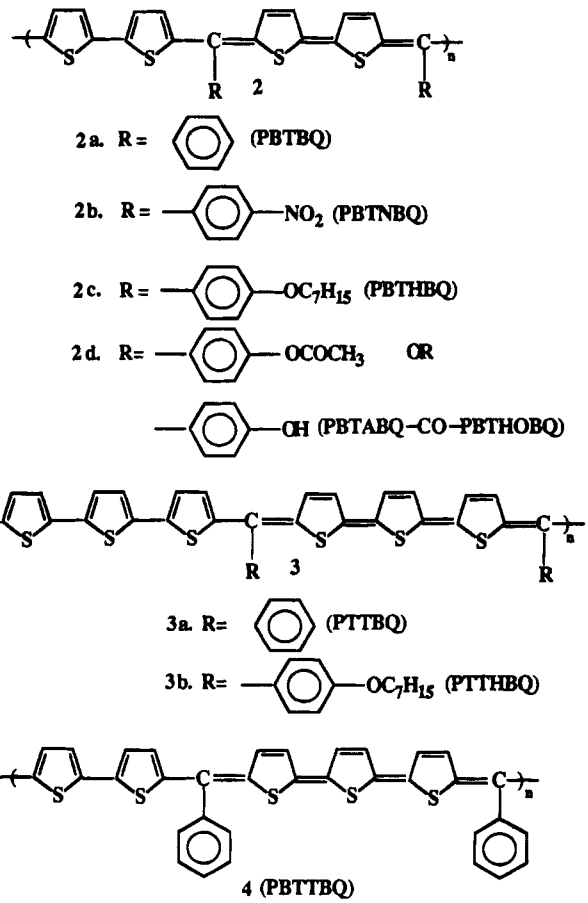

soluble in organic solvents and thus allowed an extensive characterization of the structure and properties of this class of polymers. The bulky side groups in these polymers also play an important role in improving the stability of the *quinoid* moieties in the polymers as suggested by model compound studies.[31] In part 1 of this series of reports on small-bandgap conducting polymers,[32] we reported the synthesis and characterization of the precursor poly(heteroarylene methylenes). The third-order nonlinear optical properties of some of the conjugated poly(heteroarylene methines) in Charts 1 and 2 have also been reported.[33]

Experimental Section

Materials. Tetrahydrofuran (THF) (Aldrich, anhydrous), *p*-dioxane (Aldrich, anhydrous), 1-methyl-2-pyrrolidinone (NMP) (Aldrich, anhydrous 99+%), 2,3-dichloro-5,6-dicyano-1,4-benzoquinone (DDQ) (Aldrich), sulfolane (Kodak), acetonitrile (anhydrous, 99+%), tetrabutylammonium hexafluorophosphate ($TBAPF_6$, Aldrich), 96% sulfuric acid (Baker) and ultrapure grade nitrogen gas (Air Products) were used as received. Poly[(2,5-thiophenediyl)benzylidene(2,5-thiophenequinodimethanediyl)] (PTBQ, **1a**, Chart 1), poly[(2,5-thiophenediyl)(*p*-nitrobenzylidene)(2,5-thiophenequinodimethanediyl)] (PTNQB, **1b**, Chart 1), poly(3-methylthiophene-2,5-diyl)benzylidene] (PMTB), poly(3-methylthiophene-2,5-diyl)(*p*-benzoxybenzylidene)] (PMTBB), poly(3-methylthiophene-2,5-diyl)(*p*-(heptyloxy)benzylidene)] (PMTHB), poly[(α-bithiophene-5,5′-diyl)benzylidene] (PBTB), poly[(α-bithiophene-5,5′-diyl)(*p*-nitrobenzylidene)] (PBTNB), poly[(α-bithiophene-5,5′-diyl)(*p*-(heptyloxy)benzylidene)] (PBTHB), poly[(α-bithiophene-5,5′-diyl)(*p*-acetoxybenzylidene)]-*co*-poly[(α-bithiophene-5,5′-diyl)(*p*-hydroxybenzylidene)] (PBTAB-*co*-PBTHOB), poly[(α-terthiophene-5,5′-diyl)benzylidene] (PTTB), and poly[(α-terthiophene-5,5′-diyl)(*p*-(heptyloxy)benzylidene)] (PTTHB) were synthesized by acid-catalyzed polymerization of thiophene oligomers with aldehydes.[32,34] The synthesis of 5,5″-bis(phenyl(2-thienyl)hydroxymethyl)-2,2′,5′,2″-terthiophene (named as compound **I**) will be reported elsewhere.[31]

Polymer Synthesis. Poly[(3-methylthiophene-2,5-diyl)benzylidene(3-methylthiophenequinodimethane-2,5-diyl)] (PMTBQ, 1c). The reaction mixture was 1.014 g (5.4 mmol) of PMTB, 0.247 g (1 mmol) of DDQ, and 40 mL of anhydrous THF. The reaction was maintained at 50 °C for 4 h. The dark red reaction solution was poured into 500 mL of stirring methanol, and the precipitate was recovered, extracted with hot methanol, reprecipitated from THF/methanol, and dried in a vacuum oven at 50 °C for 12 h. The yield of dehydrogenated polymer was 0.70 g (69%). IR (film on NaCl, cm^{-1}): 3056, 3020, 2950, 2920, 2850, 1676, 1597, 1576, 1492, 1443, 1381, 1321, 1292, 1176, 1137, 1109, 1074, 1029, 838, 735, 697. UV–vis (λ_{max}, THF): 226 nm ($\log \epsilon = 4.31$), 452 nm ($\log \epsilon = 3.92$). ^1H NMR (δ, ppm, TMS reference): 1.6–2.2 (6 H, $2(CH_3)$), 5.70 (0.12 H, C(R)H), 7.28 (12 H, phenyl and thiophene rings).

Poly[(3-methylthiophene-2,5-diyl)(*p*-(benzyloxy)benzylidene)(3-methylthiophenequinodimethane-2,5-diyl)] (PMTBBQ, 1d). The reaction mixture was 0.5 g (1.7 mmol) of PMTBB, 0.116 g (0.5 mmol) of DDQ, and 45 mL of anhydrous *p*-dioxane. The reaction was maintained at 78 °C for 4 h. The dark red reaction solution was poured into 500 mL of stirring methanol, and the precipitate was recovered, reprecipitated from THF/hexane, extracted with hot methanol, and dried in a vacuum oven at 70 °C for 10 h. The product was 0.41 g (82%). IR (film on NaCl, cm^{-1}): 3050, 3019, 2902, 2847, 1603, 1507, 1454, 1381, 1298, 1242, 1174, 1023, 831, 734, 696. UV–vis (λ_{max}, sulfolane): 234 nm ($\log \epsilon = 4.44$), 453 nm ($\log \epsilon = 3.92$). ^1H NMR (δ, ppm, TMS reference): 1.96 (6 H, $2(CH_3)$), 5.00 (4 H, $2(OCH_2)$), 5.65 (0.15 H, C(R)H), 6.60–7.50 (20 H, phenyl, phenylene and thiophene rings).

Poly[(3-methylthiophene-2,5-diyl)(*p*-(heptyloxy)benzylidene)(3-methylthiophenequinodimethane-2,5-diyl)] (PMTHBQ, 1e). The reaction mixture was 1.0 g (3.3 mmol of PMTHB, 0.14 g (0.6 mmol) of DDQ, and 50 mL of anhydrous THF. The reaction was maintained at 50 °C for 4 h. The dark red reaction solution was poured into 500 mL of stirring methanol, and the precipitate was recovered, extracted with hot methanol, reprecipitated from THF/methanol, and dried in a vacuum oven at 40 °C for 10 h. The yield of product was 0.65 g (65%). Anal. Calcd for $(C_{38}H_{46}S_2O_2)_n$: C , 76.68; H, 7.59; S, 10.50; O, 5.24. Found: C, 76.30; H, 7.96; S, 9.87; O, 5.46. IR (film on NaCl, cm^{-1}): 3035, 2927, 2851, 1605, 1508, 1468, 1379, 1287, 1245, 1174, 1105, 1013, 957, 831, 703. UV–vis (λ_{max}, THF): 227 nm ($\log \epsilon = 4.40$), 456 nm ($\log \epsilon = 3.76$). ^1H NMR (δ, ppm, TMS reference): 0.92 (6 H, $2(CH_3)$ on heptyloxy group), 1.33 (16 H, $2((CH_2)_4)$ on heptyloxy side chain), 1.60–2.10 (10 H, $2(OCH_2CH_2^*)$ on heptyloxy side chain and $2(CH_3)$ on the thiophene ring), 3.92 (4 H, $2(OCH_2)$), 6.8 (4 H, phenylene), 5.60 (0.13 H, C(R)H), 7.1 (6 H, phenylene and thiophene rings).

Poly[(α-(bithiophene-5,5′-diyl)benzylidene-*block*-(α-(bithiophenequinodimethane-5,5′-diyl)] (PBTBQ, 2a). The reaction mixture was 1.50 g (5.9 mmol) of PBTB, 0.67 g (3.0 mmol) of DDQ, and 60 mL of anhydrous THF. The reaction temperature was maintained at 50 °C for 10 h. A dark blue polymer was recovered in 500 mL of stirring methanol, dissolved in DMF, recovered in methanol, extracted with hot methanol in a Soxhlet apparatus, and dried in a vacuum oven at 60 °C for 12 h. The yield of product was 1.25 g (83%). Anal. Calcd for $[(C_{30}H_{18}S_4)_{0.94}(HSO_4)_{0.06}]_n$: C, 70.11; H, 3.55; S, 25.40. Found: C, 68.92; H, 3.58; S, 25.26. IR (film on NaCl, cm^{-1}): 3062, 3021, 2858, 1665, 1590, 1493, 1447, 1289, 1224, 1203, 1196, 1048, 1020, 907, 837, 795, 698. UV–vis (λ_{max}, NMP): 334 nm ($\log \epsilon = 4.33$), 429 nm ($\log \epsilon = 4.18$), 605 nm ($\log \epsilon = 4.40$). ^1H NMR (δ, ppm, TMS reference): 6.83 (4 H, phenyl), 7.10–7.40 (8 H, phenyl and aromatic thiophene rings), 7.60 (4 H, aromatic and quinoid thiophene rings), 7.90 (2 H, quinoid thiophene ring).

Poly[(α-bithiophene-5,5′-diyl)(*p*-nitrobenzylidene)-*block*-(α-bithiophenequinodimethane-5,5′-diyl)] (PBTNBQ, 2b). The reaction mixture was 1.077 g (3.6 mmol) of

PBTNB, 0.41 g (1.8 mmol) of DDQ, and 60 mL of anhydrous THF. The reaction was maintained at 57 °C for 9.5 h. The green reaction solution was poured into 500 mL of stirring hexane, and the precipitate was recovered and dissolved in 50 mL of THF. The THF-soluble and THF-insoluble fractions were separated. The THF-soluble fraction was recovered in hexane, extracted with hot methanol in a Soxhlet apparatus, recovered, and dried in a vacuum oven at 65 °C for 10 h. The THF-insoluble fraction was Soxhlet extracted with 300 mL of methanol, recovered, and dried in a vacuum oven at 65 °C for 10 h. The yield of THF-soluble fraction was 0.25 g and the yield of THF-insoluble fraction was 0.7 g (total yield = 88%). Anal. Calcd for $[(C_{30}H_{16}N_2O_4S_4)_{0.77}(HSO_4)_{0.23}]_n$: C, 57.58; H, 2.63; N, 4.48. Found: C, 58.41; H, 2.79; N, 4.31. IR (film on NaCl, cm^{-1}): 3098, 3063, 2923, 2851, 1662, 1589, 1518, 1425, 1345, 1225, 1209, 1152, 1130, 1108, 1047, 1014, 860, 846, 797, 745, 696. UV-vis (λ_{max}, NMP): 324 nm (log ϵ = 4.19), 432 nm (log ϵ = 3.89), 650 nm (log ϵ = 4.08) for the THF-soluble fraction. ^1H NMR (δ, ppm, TMS reference): 6.88 (2 H, aromatic thiophene ring), 7.00–7.40 (4 H, aromatic thiophene and quinoid thiophene rings), 7.60 (4 H, phenylene), 7.80 (2 H, quinoid thiophene ring), 8.23 (4 H, phenylene).

Poly[α-(bithiophene-5,5′-diyl)-(*p*-(heptyloxy)benzylidene)-*block*-(α-bithiophenequinodimethane-5,5′-diyl)] (PBTHBQ, 2c). The reaction mixture was 0.50 g (1.4 mmol) of PBTHB, 0.15 g (0.7 mmol) of DDQ, and 45 mL of anhydrous *p*-dioxane. The reaction was maintained at 80 °C for 10 h. The dark blue reaction solution was poured into 500 mL of stirring methanol, and the precipitate was recovered, reprecipitated from THF/hexane, extracted with hot methanol in a Soxhlet apparatus, and dried in a vacuum oven at 70 °C for 10 h. The yield of product was 0.37 g (74%). Anal. Calcd for $[(C_{44}H_{46}S_4O_2)_{0.75}(HSO_4)_{0.25}]_n$: C, 68.86; H, 6.09; S, 18.10; O, 6.95; N, 0. Found: C, 67.81; H, 5.75; S, 17.89; O, 7.53; N, 0.14. IR (film on NaCl, cm^{-1}): 3055, 2927, 2855, 1646, 1602, 1508, 1467, 1438, 1294, 1251, 1174, 1125, 1052, 839, 799, 756, 695. UV–vis (λ_{max}, THF): 337 nm (log ϵ = 4.16), 582 nm (log ϵ = 4.17). ^1H NMR (δ, ppm, TMS reference): 0.91 (6 H, 2(CH_3)), 1.40 (16 H, 2((CH_2)$_4$)), 1.85 (4 H, 2(OCH_2CH_2*) on heptyloxy side chain), 4.00 (4 H, 2(OCH_2)), 6.86 (4 H, phenylene), 7.00 (4 H, phenylene), 7.13 (2 H, aromatic thiophene ring), 7.26 (2 H, aromatic thiophene ring), 7.43 (2 H, quinoid thiophene rings), 7.90 (2 H, quinoid thiophene ring).

PBTHBQ1. The synthetic procedures and purification of this polymer are the same as for the preparation of PBTHBQ. The reaction mixture was 0.4 g (1 mmol) of PBTHB, 25 mg (0.1 mmol) of DDQ, and 40 mL of anhydrous *p*-dioxane. The reaction was maintained at 80 °C for 8 h. The yield of product was 0.32 g (80%). IR (film on NaCl, cm^{-1}): 3055, 2952, 2927, 2856, 1646, 1605, 1582, 1509, 1467, 1439, 1301, 1251, 1175, 1111, 1024, 963, 900, 865, 836, 799, 756, 694. UV–vis (λ_{max}, THF): 326 nm (log ϵ = 4.23), 567 nm (log ϵ = 3.53). ^1H NMR (δ, ppm, TMS reference): 0.91, 1.40, 1.85, 4.00, 5.71, 6.86, 7.00, 7.13, 7.26, 7.43, 7.90.

PBTHBQ2. The synthetic procedures and purification of this polymer are the same as for the preparation of PBTHBQ. The reaction mixture was 0.40 g (1 mmol) of PBTHB, 49 mg (0.2 mmol) of DDQ, and 40 mL of anhydrous *p*-dioxane. The reaction was maintained at 80 °C for 9 h. The yield of product was 0.32 g (80%). IR (film on NaCl, cm^{-1}): 3032, 2953, 2927, 2850, 1653, 1602, 1509, 1467, 1430, 1300, 1249, 1174, 1125, 1050, 1012, 837, 799, 756, 693. UV–vis (λ_{max}, THF): 326 nm (log ϵ = 4.19), 588 nm (log ϵ = 3.76). ^1H NMR (δ, ppm, TMS reference): 0.91, 1.40, 1.85, 4.00, 5.71, 6.86, 7.00, 7.13, 7.26, 7.43, 7.90.

PBTHBQ3. The synthetic procedures and purification of this polymer are the same as for the preparation of PBTHBQ. The reaction mixture was 0.4 g (1 mmol) of PBTHB, 64 mg (0.4 mmol) of DDQ, and 40 mL of anhydrous *p*-dioxane. The reaction was maintained at 80 °C for 8 h. The yield of product was 0.33 g (82.5%). IR (film on NaCl, cm^{-1}): 3070, 2927, 2855, 1646, 1602, 1508, 1467, 1430, 1300, 1249, 1174, 1125, 1049, 837, 799, 693. UV–vis (λ_{max}, THF): 325 nm (log ϵ = 4.22), 593 nm (log ϵ = 4.06). ^1H NMR (δ, ppm, TMS reference): 0.91, 1.40, 1.85, 4.00, 5.71, 6.86, 7.00, 7.13, 7.26, 7.43, 7.90.

Poly[(α-(bithiophene-5,5′-diyl)(*p*-acetoxybenzylidene)-*block*-(α-bithiophenequinodimethane-5,5′-diyl)]-*co*-poly-[(α-bithiophene-5,5′-diyl)(*p*-hydroxybenzylidene)-*block*-(α-bithiophenequinodimethane-5,5′-diyl)] (PBTABQ-*co*-PBTHOBQ, 2d). The reaction mixture was 0.5 g (1.8 mmol) of PBTAB-*co*-PBTHOB, 0.18 g (0.8 mmol) of DDQ, and 50 mL of anhydrous THF. The reaction was maintained at 55 °C for 2 h. The dark blue solution was poured into 500 mL of stirring hexane, and the precipitate was recovered, extracted with methanol in a Soxhlet apparatus, and dried in a vacuum oven at 50 °C for 12 h. The product was 0.42 g (84%). IR (film on NaCl, cm^{-1}): 3370, 3060, 1660, 1601, 1511, 1414, 1384, 1304, 1277, 1225, 1170, 1139, 1053, 795, 724. UV–vis (λ_{max}, DMF): 527 nm (log ϵ = 4.30), 329 nm (log ϵ = 4.38). ^1H NMR (δ, ppm, TMS reference): 2.30 (0.26 H, CH_3 on acetoxy side group), 6.80 (6.96 H, phenylene ring with hydroxy side group), 7.12 (3.48 H, aromatic thiophene ring (hydroxy side group)), 7.35 (3.48 H, quinoid thiophene ring (hydroxy side group)), 7.50 (0.52 H, phenylene ring with acetoxy side group), 7.60–7.90 (0.52 H, quinoid thiophene ring (acetoxy side group)).

Poly[(α-bithiophene-5,5′-diyl)benzylidene-*block*-(α-terthiophenequinodimethane-5,5′-diyl)] (PBTTBQ, 4). The reaction mixture was 1.34 g (2 mmol) of 5,5″-bis(phenyl(2-thienyl)hydroxymethyl)-2,2′,5′,2″-terthiophene (compound **I**), 1 g (21.7 mmol) of formic acid, and 45 mL of THF. The reaction was kept at 50 °C for 10 h. The deep green reaction mixture was poured into an 800 mL beaker containing 20 g of sodium bicarbonate and 400 mL of deionized water. This solution was extracted with THF and then dried over Na_2SO_4, the solvent was evaporated, and a deep green product was obtained. The product was further purified by reprecipitation from THF/hexane and dried in a vacuum oven at 50 °C for 12 h. The yield was 51%. FTIR (film on NaCl, cm^{-1}): 3056, 3021, 2971, 2859, 1647, 1584, 1485, 1436, 1379, 1288, 1217, 1147, 1048, 1027, 985, 879, 781, 745, 689. UV–vis (λ_{max}, THF): 631 nm (log ϵ = 4.27), 449 nm (log ϵ = 4.23), 389 nm (log ϵ = 4.21 M^{-1} cm^{-1}). ^1H NMR (δ, ppm, TMS reference): 6.40, 6.72, 6.83, 6.95, 7.15, 7.35, 7.40.

Attempted Synthesis. Poly[(α-terthiophene-5,5″-diyl)-benzylidene-*block*-(α-terthiophenequinodimethane-5,5″-diyl)] (PTTBQ, 3a). The reaction mixture was 0.75 g (2.2 mmol) of PTTB, 0.33 g (1.5 mmol) of DDQ, and 40 mL of anhydrous THF. The reaction was maintained at 50 °C for 2 h. The dark green solution was poured into 500 mL of stirring hexane, and the precipitate was recovered, extracted with hot methanol, and dried in a vacuum oven at 50 °C for 12 h. The yield of product was 0.6 g (80%). IR (film on NaCl, cm^{-1}): 3056, 2964, 2858, 1626, 1590, 1506, 1491, 1430, 1361, 1287, 1221, 1176, 1139, 1049, 907, 830, 788, 696. UV–vis (λ_{max}, THF): 381 nm (log ϵ = 4.58), 687 nm (log ϵ = 3.83). ^1H NMR (δ, ppm, TMS reference): 6.1 (0.09 H, C(R)H), 6.93, 7.18, 7.20–7.50, 7.50–7.80.

Poly[α-(terthiophene-5,5″-diyl)(*p*-(heptyloxy)benzylidene)-*block*-(α-terthiophenequinodimethane-5,5″-diyl)] (PTTHBQ, 3b). The reaction mixture was 0.656 g (1.5 mmol) of PTTHB, 0.23 g (1 mmol) of DDQ, and 40 mL of anhydrous THF. The reaction mixture was maintained at 50 °C for 2 h. The dark green solution was poured into 400 mL of stirring hexane, and the precipitate was recovered, reprecipitated from THF/hexane, extracted with hot methanol in a Soxhlet apparatus, and dried in a vacuum oven at 50 °C for 12 h. The yield of product was 0.41 g (63%). Anal. Calcd for $[(C_{52}H_{50}S_6O_2)_{0.82}(HSO_4)_{0.18}]_n$: C, 67.84; H, 5.50; S, 21.66; O, 5.00. Found: C, 65.09; H, 5.19; S, 21.44; O, 6.65. IR (film on NaCl, cm^{-1}): 3070, 2922, 2851, 1626, 1600, 1569, 1508, 1432, 1368, 1290, 1253, 1173, 1139, 966, 839, 794, 756, 694. UV–vis (λ_{max}, THF): 667 nm (log ϵ = 4.00), 381 nm (log ϵ = 4.68). ^1H NMR (δ, ppm, TMS reference): 0.93 (6 H, 2(CH_3)), 1.30 (16 H, 2((CH_2)$_4$)), 1.75 (4 H, 2(OCH_2CH_2*) on heptyloxy side chain), 4.0 (4 H, 2(OCH_2)), 6.90, 6.97 (4 H, phenylene), 7.10–7.40, 7.50, 7.95.

Characterization. Infrared spectra of polymer thin films cast on NaCl windows from THF or DMF solutions were recorded at room temperature using a Nicolet Model 20 SXC FTIR spectrometer. The ^1H NMR spectra were obtained in

deuterated methylene chloride (CD_2Cl_2), chloroform ($CDCl_3$), dimethyl sulfoxide (DMSO-d_6), or dimethylformamide (DMF-d_7) with a General Electric Model QE300 instrument. Elemental analysis was done by Galbraith Laboratories, Inc. (Knoxville, TN), or Oneida Research Services, Inc. (Whitesboro, NY). Electronic absorption spectra of polymer solutions or thin films were obtained at room temperature in the wavelength range 185–3200 nm with a Perkin-Elmer Lambda 9 UV–vis–near-IR spectrophotometer. Thin films of polymers were cast from 2–3 wt % polymer solutions by spin coating at a speed of 4000 rpm for 1 min. Thermal analysis, differential scanning calorimetry (DSC), and thermogravimetric analysis (TGA) were done by using a Dupont Model 1090B thermal analyzer or a Dupont Model 2100 thermal analysis system based an IBM PS/2 Model 60 computer under a flowing nitrogen atmosphere. Indium (156.4 °C) standard was used to calibrate the accuracy of measured transition points. Samples were sealed in DSC pans and run at 20 °C/min under flowing nitrogen. TGA runs were performed at a heating rate of 10 °C/min under flowing nitrogen. Intrinsic viscosities, $[\eta]$, of all polymers in DMF were determined at 30 °C with a Cannon Ubbelohde capillary viscometer and a constant-temperature bath. The intrinsic viscosity values were extracted from the zero-concentration extrapolation of the intersection of plots of the reduced viscosity (η_{sp}/C) and inherent viscosity ($\eta_{inh} = [\ln \eta_{rel}]/C$) versus concentration.

ESR spectra were recorded on a Bruker EP 300 spectrometer equipped with a dual microwave cavity. Diphenylpicrylhydrazyl (DPPH) was used as a reference for determination of g-values. A standard solution of 4-hydroxy-2,2,6,6-tetramethylpiperidinyloxy (4-hydroxy-TEMPO) in THF was used in the determination of spin concentrations. The concentration of the standard solution was 3.997×10^{-4} M. The measurement was performed at room temperature. ESR samples (5–10 mg) were prepared in quartz sample tubes in a drybox under a nitrogen atmosphere. The preparation of the ESR samples for the study of the mechanism of the dehydrogenation reaction was as follows. PBTHB (0.3 g) was dissolved in 40 mL of anhydrous THF, and DDQ (74 mg) was added to this solution. This mixture was magnetically stirred at 50 °C in a drybox under a nitrogen atmosphere. ESR spectra of this mixture were recorded as a function of time and under the same experimental conditions (i.e., the time constant, modulus amplitude, and receiver gain were kept the same), and a standard solution was used to determine the spin concentrations.

The electrochemical properties of films of the polymers were studied by cyclic voltammetry. For cyclic voltammetry, an electrolyte solution of 0.1 M tetrabutylammonium hexafluorophosphate ($TBAPF_6$) in acetonitrile was used in the experiments. Platinum wire electrodes were used as both counter and working electrodes and silver/silver ion (Ag in 0.1 M $AgNO_3$ in the electrolyte solution, from Bioanalytical Systems, Inc.) was used as a reference electrode. The polymers were coated onto the working electrode by dipping the Pt wire electrode into 10–15% THF or DMF solutions of the polymers. Each coated electrode was dried in a vacuum oven at 60 °C for 2 h. The reference electrode was calibrated at the beginning of each experiment by running cyclic voltammetry on ferrocene as the standard in an identical cell without any polymer on the working electrode. The electrochemical equipment used for the experiments was an EG&G Princeton Applied Research Model 273 potentiostat/galvanostat. Data were collected and analyzed by using a Model 270 Electrochemical Analysis System for Model 273 from the same company. The potential values obtained versus ferrocene were converted to versus saturated calomel electrode (SCE) by adding a constant of 0.1588 V to them. The conversion is based on the reduction potentials[35] of ferrocenium/ferrocene (Fc^+/Fc) (0.4 V versus NHE, normal hydrogen electrode) and SCE (0.2412 V versus NHE). Thus, the reduction potential of Fc^+/Fc versus SCE is 0.1588 V.

The gas-phase ionization potential (IP) and electron affinity (EA) of the polymers were estimated using the following relations:[36] $[E_{on}]^{ox} = IP - 6.3$ and $[E_{on}]^{red} = EA - 6.3$, where $[E_{on}]^{ox}$ and $[E_{on}]^{red}$ are the onset potentials for the oxidation and reduction of the polymers versus SCE. Solid-state IP and EA values were obtained by subtracting the polarization energy, 1.9 eV, from the gas-phase values.[36–38]

Iodine doping of PBTBQ, PBTHBQ, and PBTNBQ films was achieved as follows. Thin films of the polymers on glass substrates were placed into a jar containing iodine vapor and sealed for 30 min. The iodine-doped polymer films were removed and placed in a vacuum oven at 60 °C for 3 h to remove any excess iodine from the sample. The doping process was repeated until no further change in conductivity was observed. The degree of doping was determined from the weight difference between the undoped and doped samples, and the amount of iodine uptake was considered to be I_3^-. The conductivity of the polymer thin films was measured with a standard four-point technique in air at room temperature by using a Keithley Model 220 current source and a Model 617 electrometer as a voltmeter.

Scheme 1

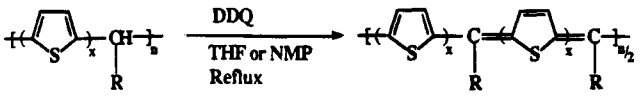

Table 1. Amount of DDQ Used in Scheme 1 and Degree of Dehydrogenation of Poly(heteroarylene methines)

polymer	DDQ/repeat unit	% dehydrogenation
PTBQ	–	100
PTNBQ	–	100
PMTBQ[a]	0.2	88
PMTBBQ[a]	0.3	85
PMTHBQ[a]	0.2	87
PBTBQ	0.5	100
PBTNBQ	0.5	100
PBTHBQ1	0.1	20
PBTHBQ2	0.2	40
PBTHBQ3	0.28	54
PBTHBQ	0.5	100
PBTABQ-*co*-PBTHOBQ	0.5	100
PBTTBQ	–	–

[a] PMTB, PMTBB, and PMTHB were 64, 58, and 62% dehydrogenated as synthesized.

Results and Discussion

Synthesis and Structure. Poly(heteroarylene methines) **1** and **2** were prepared by the dehydrogenation reaction of precursor poly(thienylene methylenes) with 2,3-dichloro-5,6-dicyano-1,4-benzoquinone (DDQ) in solution as represented by Scheme 1. Theoretically, 1 mol of a precursor polymer repeat unit requires 0.5 mol of DDQ to produce a completely dehydrogenated polymer repeat unit. As expected, 0.5 mol of DDQ was required to completely dehydrogenate the precursors leading to PBTBQ (**2a**), PBTNBQ (**2b**), PBTHBQ (**2c**), or PBTABQ-*co*-PBTHOBQ (**2d**). Since some of the precursor poly(thienylene methylenes) were already partially dehydrogenated as synthesized by acid-catalyzed polymerization (e.g., 64, 58, and 62% for PMTB, PMTBB, and PMTHB, respectively), a proportionately smaller amount of DDQ was required to achieve dehydrogenation. However, the resulting poly(thienylene methines), PMTBQ, PMTBBQ, and PMTHBQ were found to be only 85–88% dehydrogenated as shown in Table 1. The reason for the less than 100% dehydrogenation of some of the poly(thienylene methines) **1** is due largely to the methine hydrogen of the polymer end groups that is still detectable by ^1H NMR in these low molecular weight polymers. The degree of dehydrogenation was determined from the integration peak of the methine hydrogen resonance in the ^1H NMR spectra, and the results

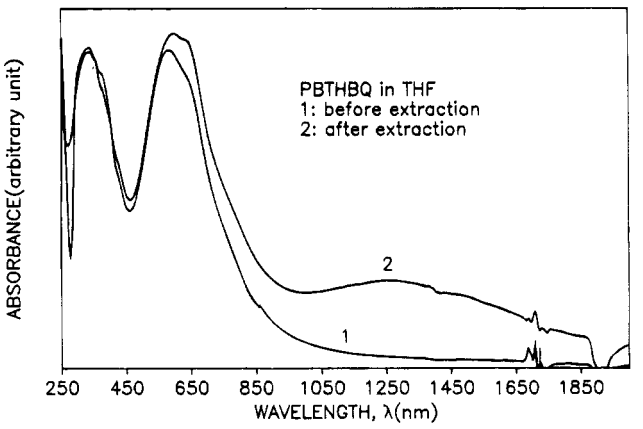

Figure 1. Optical absorption spectra of PBTHBQ in THF: (1) before purification; (2) after purification.

for all the polymers are collected in Table 1. An interesting feature of the synthesis of poly(bithienylene methines) **2** was the accurate control of the degree of dehydrogenation by the amount of DDQ used. For example, by using the mole ratio of DDQ to PBTHB repeat unit equal to 0.1, 0.2, 0.28, and 0.5, the degree of dehydrogenation on PBTHB is found to be 20, 40, 54, and 100%, respectively. The partially dehydrogenated polymers contain a varying conjugation length in the polymer backbone as evidenced by the optical absorption spectra to be discussed later. Hence, conjugation length as well as electronic and optical properties of PBTHBQ could be controlled by the amount of DDQ used in the dehydrogenation reaction.

Some of the freshly prepared poly(bithienylene methines) were slightly doped by DDQ before they were purified by extraction with hot methanol or acetone in a Soxhlet apparatus. For example, the optical absorption spectrum of a THF solution of a freshly prepared PBTHBQ shows a strong absorption band at 582 nm ($\log \epsilon = 4.19$) and a small broad band at 1253 nm ($\log \epsilon = 3.31$) as exhibited in Figure 1. The band at 582 nm is clearly due to the pure polymer. The band at 1253 nm in the near-infrared region is due to doping or the effect of impurity DDQ on PBTHBQ since extraction of the "partially doped" PBTHBQ with methanol in a Soxhlet apparatus results in the complete disappearance of the absorption band at 1253 nm. This suggests that the DDQ-doped PBTHBQ is not stable. A similar dedoping phenomenon was previously observed with $FeCl_3$-doped poly(3-alkylthiophenes)[39] and poly[3-(alkyloxy)thiophenes].[40] The optical absorption spectra of the freshly prepared PBTBQ and PBTABQ-*co*-PBTHOBQ in NMP solutions also showed a very small broad absorption band in the near-infrared region before thorough extraction with methanol. This near-IR absorption band also completely disappeared after extraction with methanol in a Soxhlet apparatus. The lack of DDQ impurities in these polymers was further confirmed by the FTIR and elemental analysis results which will be discussed later. Hence, the neutral and pure poly(bithienylene methines) **2** have been successfully prepared in accord with Scheme 1.

We also attempted to prepare poly(α-terthienylene methines) **3** by Scheme 1. Although the dehydrogenation reaction of the precursor PTTB and PTTHB with DDQ did occur as evidenced by their ^1H NMR spectra, the products were not consistent with the expected structure. The proton number of the thiophene ring was lower than expected. Elemental analysis of PTTHBQ

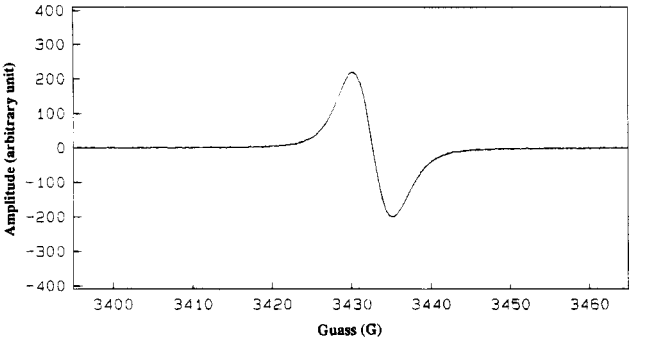

Figure 2. ESR spectrum of PBTHBQ/DDQ mixture 5 h after PBTHB was mixed with DDQ.

(**3b**) showed an oxygen content that was 1.65% higher than its precursor PTTHB. The optical absorption spectrum of PTTHBQ exhibited a visible absorption band with a moderate extinction coefficient ($\log \epsilon = 4$). These results suggest that PTTHBQ probably reacted with DDQ or oxygen or both during the dehydrogenation reaction or purification process. The expected very low ionization potential of PTTHBQ may be the reason for this. The failure to obtain PTTBQ (**3a**) by the same scheme may also be explained by the same reason, i.e., low ionization potential. An alternative reaction scheme was used to synthesize poly(heteroarylene methines) containing a terthienylene segment with quinoid geometry, as shown in Scheme 2. The polymer (PBTTBQ, **4**) had a deep green color and a very strong absorption band in the visible region. The spectroscopic characterization shows that this polymer has the expected structure.

Electron spin resonance (ESR) spectroscopy was used to probe the possible intermediates of the polymer dehydrogenation reactions with DDQ. Dehydrogenation reactions with DDQ are generally ionic reactions.[29,30] However, radical intermediates are also known in some cases.[41-43] For example, the dehydrogenation of bilirubin to biliverdin with DDQ was shown to occur via a radical intermediate.[42] The preparation of poly(4,4′-diphenylimine methines) from poly(4,4′-diphenylamine methylenes) was also shown to be through radical intermediates.[43] PBTHB and DDQ separately did not show any ESR signal. However, when mixed together, they showed an ESR signal. This means that a radical species was produced in the mixture. Figure 2 shows the ESR spectrum of the PBTHBQ/DDQ reaction mixture after PBTHB was mixed with DDQ for 5 h. The ESR signal is localized at $g = 2.005948$, has a line width of 3.6 G, and gives a spin concentration of 1 spin per 28 repeat units. The spin concentration was found to decrease rapidly with time. These results clearly indicate that a radical species was a reaction intermediate when PBTHB was oxidized with DDQ and that the dehydrogenation reaction proceeded with a radical intermediate.

Table 2 shows the results of the ESR study of the poly(heteroarylene methines). PTBQ, PTNBQ, PMTBQ, PMTBBQ, PMTHBQ, and PBTTBQ did not show any ESR signal. However, the other conjugated polymers exhibit singlet ESR signals. The spin concentrations are in the range of 4×10^{17}–5.8×10^{18} spin/g (1 spin per 174 structural units to 1 spin per 2778 structural units). Since the spin concentration of these conjugated polymers is low, this rules out the possible diradical structure which was proposed for this class of polymers earlier.[33c] The spin concentrations of these polymers are comparable with or smaller than those of neutral

Table 2. ESR Results for Poly(heteroarylene methines)

polymer	spin/gram	spin/unit[a]	*g*-value	ΔH_{pp} (G)
PTBQ[b]	–	–	–	–
PTNBQ[b]	–	–	–	–
PMTBQ[b]	–	–	–	–
PMTBBQ[b]	–	–	–	–
PMTHBQ[b]	–	–	–	–
PBTBQ	3.86×10^{18}	0.00325	2.005957	2.6
PBTNBQ	5.81×10^{18}	0.00576	2.004987	3.6
PBTHBQ	2.24×10^{18}	0.00274	2.006034	5.1
PBTABQ-*co*-PBTHOBQ	4×10^{17}	0.00036	2.006097	4.1
PBTTBQ	4.82×10^{18}	0.00471	2.003714	7.3

[a] The repeat unit of polymer. [b] ESR was not detected.

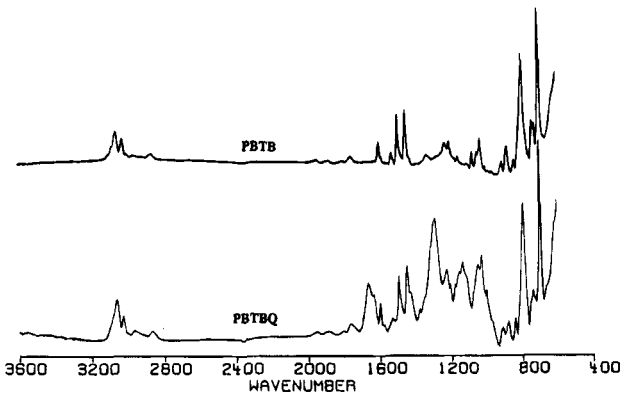

Figure 3. FTIR absorption spectra of PBTB and PBTBQ.

conjugated polymers such as *trans*-polyacetylene (10^{19} spin/g),[44a] polythiophene (3.3×10^{17} spin/g),[44a] polypyrrole (2×10^{19} spin/g),[44b] poly(*p*-phenylene) ($\sim 10^{19}$ spin/g),[44a] and poly(*p*-phenylenevinylene) (5.9×10^{17} spin/g).[44c]

Figure 3 shows the FTIR spectra of precursor PBTB and its completely dehydrogenated derivative PBTBQ. The α-linkage of these materials is identified from the strong absorption band around 800 cm^{-1}, which is due to the C_β–H out-of-plane vibration and is characteristic of an α-linkage in the thiophene ring (794 cm^{-1} for PBTB and 795 cm^{-1} for PBTBQ). In the FTIR spectrum of PBTB, the absorption bands at 1450 and 1493 cm^{-1} are assigned to the overlap of the C=C antisymmetric and symmetric stretching vibration band of the aromatic thiophene ring. This assignment is based on the reported IR spectra of thiophene oligomers and polythiophene by Furukama et al.[45] The absorption band at 1590 cm^{-1} is due to the C=C ring stretching vibration band of the phenyl ring at the bridge carbon. The methine bridge C–H stretching vibration band of PBTB is shown in the region 2800–3000 cm^{-1}. In the FTIR spectrum of conjugated PBTBQ, the stretching vibration bands due to the aromatic thiophene ring and phenyl ring are still observed at 1450 and 1490 cm^{-1} and 1590 cm^{-1}, respectively. However, a strong new band at 1665 cm^{-1} is found and can be assigned to the C=C stretching vibration band of the quinoid bithiophene ring from our previous study of the model compound of PBTBQ.[31] Another major change in converting PBTB to PBTBQ is that the methine bridge C–H stretching vibration bands around 2800–3000 cm^{-1} in the PBTB spectrum are significantly modified in the spectrum of PBTBQ. These FTIR spectral results suggest that PBTB has been successfully dehydrogenated to PBTBQ by DDQ and are consistent with the proposed structure of PBTBQ.

Figure 4 shows the FTIR spectra of precursor PBTHB,

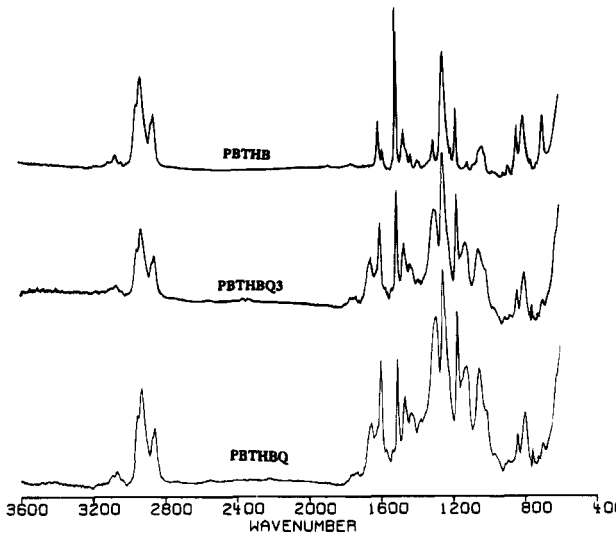

Figure 4. FTIR absorption spectra of PBTHB, PBTHBQ3, and PBTHBQ.

the 54% dehydrogenated PBTHBQ3, and the fully dehydrogenated PBTHBQ. Among the many changes observed in the spectrum of precursor PBTHB is the appearance of a new band at 1646 cm^{-1} in PBTHBQ3 and PBTHBQ. This band is characteristic of the C=C ring stretching vibration band of the quinoid bithienylene ring and clearly suggests the dehydrogenation of the precursor polymer. In other dehydrogenated polymers, the C=C stretching vibration band of the quinoid thienylene ring was found in PBTNBQ (1662 cm^{-1}), PBTABQ-*co*-PBTHOBQ (1660 cm^{-1}), and PBTTBQ (1647 cm^{-1}). However, the expected stretching vibration band of the quinoid thienylene ring near 1660 cm^{-1} could not be unambiguously assigned in poly(thienylene methines) **1** because of the overlap of the phenyl or phenylene ring stretching band in this region. The characteristic peaks of DDQ (C=N at 2210 cm^{-1} and C=O at 1750 cm^{-1}) or the byproduct of the dehydrogenation reaction, 2,3-dichloro-5,6-dicyano-1,4-hydroquinone (DDHQ, 3264 cm^{-1}), were not observed in the FTIR spectra of these dehydrogenated polymers. This means that DDQ or DDHQ impurity is absent or negligible in these dehydrogenated polymers. A comparison of the FTIR spectra of the diol monomer (compound **I**) with the polymer PBTTBQ showed that the O–H vibration band observed at 3535 cm^{-1} in the monomer was completely absent in the polymer. Furthermore, the characteristic C=C stretching band of the quinoid terthienylene ring was observed at 1647 cm^{-1} in the FTIR spectrum of PBTTBQ. These results confirm the successful synthesis of PBTTBQ from compound **I** as represented in Scheme 2. The assignment of the main bands of the poly(heteroarylene methines) is summarized in Table 3. The overall conclusion from the FTIR spectra is that they are in good agreement with the proposed structures of Charts 1 and 2.

A detailed ^1H NMR investigation of the structures of the poly(heteroarylene methines) was made possible by their solubilities in organic solvents. Figure 5 shows the ^1H NMR spectra of precursor PBTB (Figure 5a) in $CDCl_3$ (solvent peak at $\delta = 7.27$ ppm is marked "x") and the dehydrogenated conjugated polymer PBTBQ (Figure 5b) in DMF-d_8 (solvent peak near 8 ppm is marked "x"). The characteristic methine hydrogen resonance is observed at 5.95 ppm in PBTB but has completely disappeared in PBTBQ, suggesting that the precursor poly-

Scheme 2

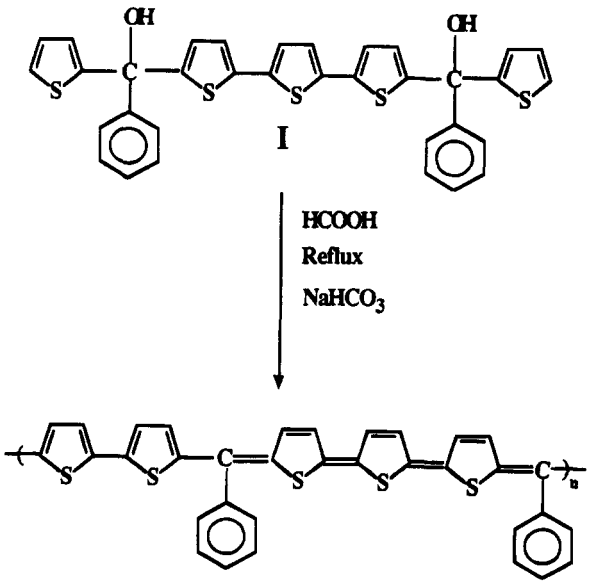

Table 3. Assignment of the FTIR Spectra of Poly(heteroarylene methines) (cm^{-1})

polymer	out-of-plane C−H bending	aromatic C=C thiophene ring stretching	phenyl or phenylene C=C ring stretching
P3HT	822	1457, 1508	—
PTBQ	801	1443, 1492	1598
PTNBQ	794	1440, 1491	1593
PMTBQ	838	1443, 1492	1576, 1597
PMTBBQ	831	1454, 1507	1603
PMTHBQ	831	1468, 1508	1605
PBTBQ	795	1447, 1493	1590
PBTNBQ	797	1425, 1518	1589
PBTHBQ	799	1438, 1467, 1508	1602
PBTABQ-*co*-PBTHOBQ	795	1414, 1511	1601
PBTTBQ	781	1436, 1485	1584

mer has been successfully converted to the conjugated polymer PBTBQ by oxidative dehydrogenation with DDQ. The assignment of the other proton resonances in PBTB and PBTBQ are indicated in Figure 5. The ^1H NMR spectra of precursor PBTHB, a partially dehydrogenated derivative PBTHBQ3, and the fully dehydrogenated conjugated polymer PBTHBQ in CD_2Cl_2 are shown in Figure 6a−c (solvent peak at $\delta = 5.35$ ppm is marked "x" as is impurity water in CD_2Cl_2 at 1.6 ppm). Two major changes in the NMR spectrum of precursor PBTHB, as it is gradually converted to the conjugated polymer PBTHBQ, are noteworthy. First, the characteristic methine proton resonance at 5.7 ppm decreases in intensity in PBTHBQ3 and completely disappears in PBTHBQ. This gradual elimination of the methine proton resonance is consistent with the amount of DDQ used in the dehydrogenation reactions. The mole ratio of DDQ to precursor polymer repeat unit used in the synthesis of PBTHBQ3 and PBTHBQ was 0.28 and 0.50, respectively, corresponding to theoretically expected 56 and 100% degrees of dehydrogenation. The actual measured degrees of dehydrogenation from the NMR spectra were 54 and 100% for PBTHBQ3 and PBTHBQ, respectively. Clearly, the degree of dehydrogenation can be accurately controlled. A second major change is the observation of new proton resonances in the 7.5−7.9 ppm range that were absent in the NMR spectrum of PBTHB. These new resonances which are due to the formation of the quinoid rings in the polymer backbone increased in intensity with increasing degree

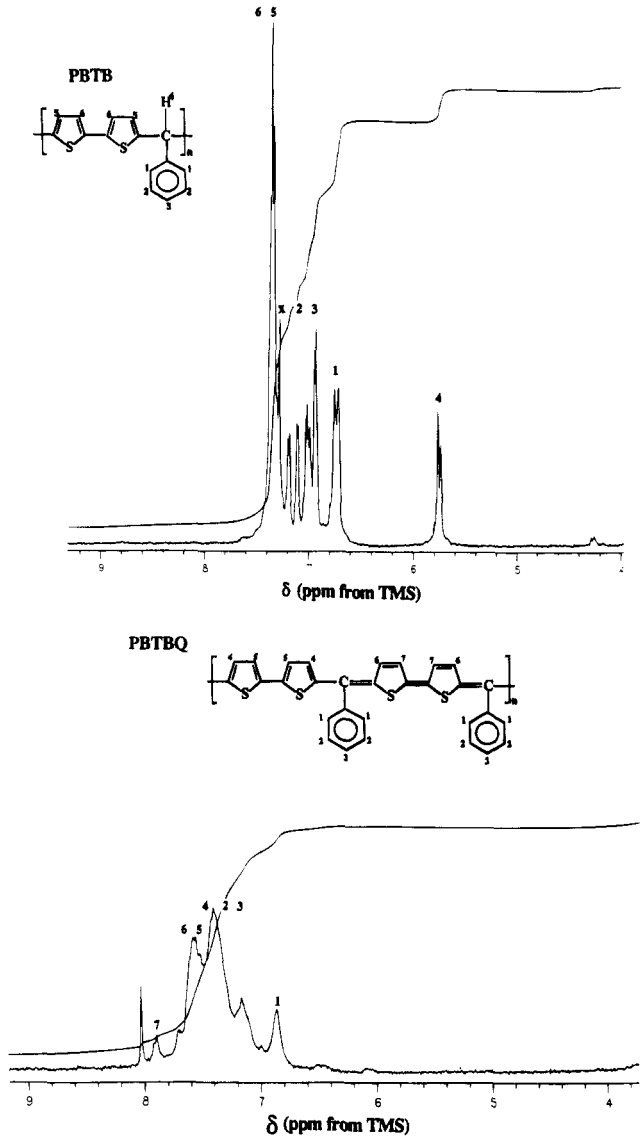

Figure 5. ^1H NMR spectra of (a) PBTB (in $CDCl_3$) and (b) PBTBQ (in DMF-d_8).

of dehydrogenation. These results exemplify the successful dehydrogenation of precursor poly(heteroarylene methylenes) by DDQ to give conjugated poly(heteroarylene methines). The assignment of the ^1H NMR spectra of all the poly(heteroarylene methines) is reported in the Experimental Section.

Finally, elemental analysis was done on selected polymers to confirm the structures of the poly(heteroarylene methines). The results of the elemental analysis of the dehydrogenated conjugated polymers were in good agreement with the expected structures. Since the molecular weights of these polymers are low ($M_w = 2500-10000$), it is necessary to take the effect of the end groups such as HSO_4 into account (this end group comes from acid-catalyzed polymerization used in the preparation of the precursor polymers[32]). The analytical data for the poly(heteroarylene methines) did not show the existence of any significant amount of DDQ or byproduct DDHQ.

Solution Properties and Intrinsic Viscosity. Most of the conjugated poly(heteroarylene methines) were found to be soluble in organic solvents. For example, PTBQ, PTNBQ, PMTBQ, PMTBBQ, PMTHBQ, and PBTTBQ are soluble in THF or DMF up to 20 wt %. This high solubility is due to the low molecular weight

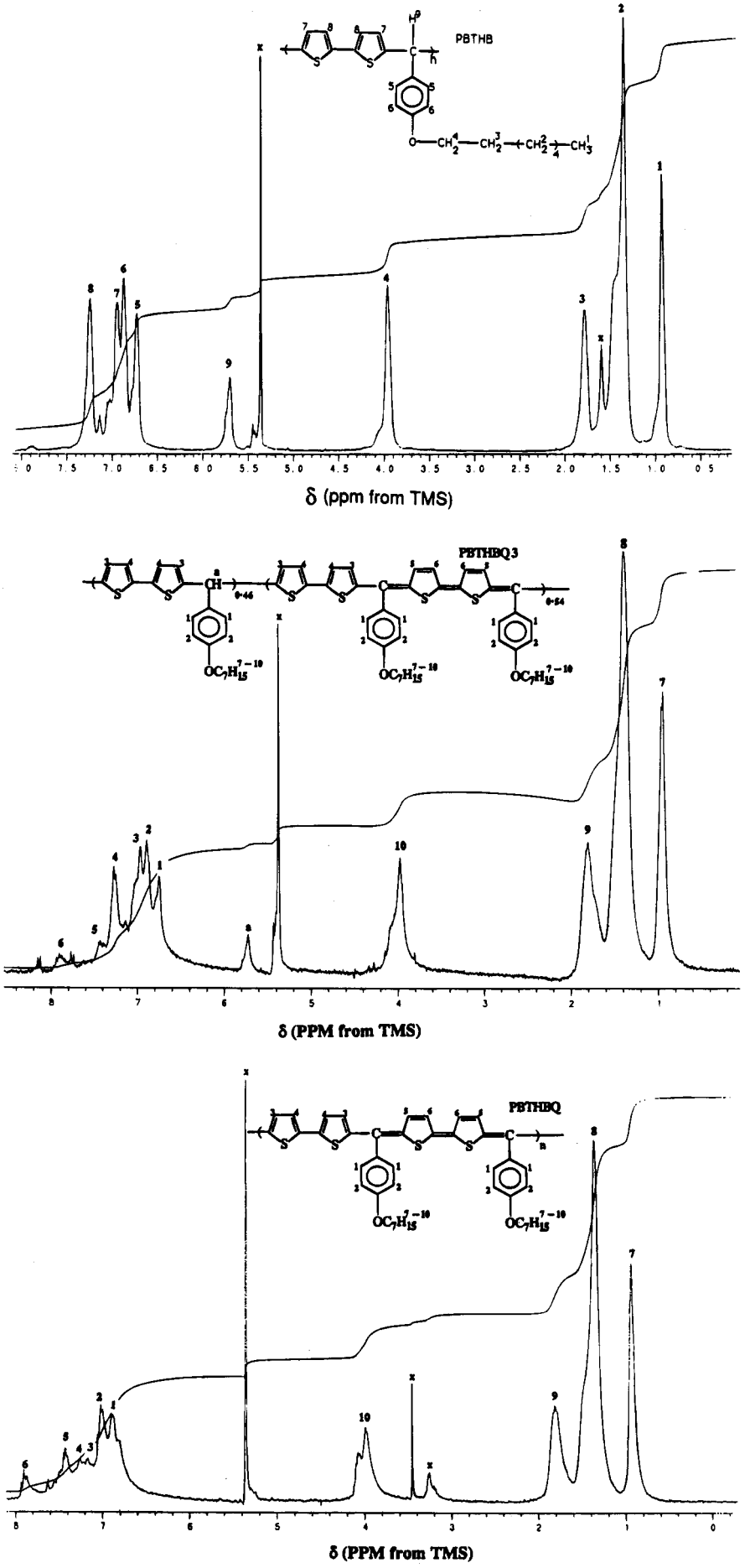

Figure 6. ^{1}H NMR spectra of (a) PBTHB (in CD_2Cl_2), (b) PBTHBQ3 (in CD_2Cl_2), and (c) PBTHBQ (in CD_2Cl_2).

Table 4. Properties of Poly(heteroarylene methines)

polymer	$[\eta]^a$ (dL/g)	$T_d{}^b$ (°C)	T_g (°C)
P3HT	0.445[c]	360	19
PTBQ	0.046	375	138
PTNBQ	0.042	300	*f*
PMTBQ	0.051	365	*f*
PMTBBQ	0.060	300	104
PMTHBQ	0.060	350	*f*
PBTBQ	0.183[d]	370	*f*
PBTNBQ	0.059[d]	300	*f*
PBTHBQ1	*e*	360	25
PBTHBQ2	*e*	360	33
PBTHBQ3	*e*	360	*f*
PBTHBQ	0.065	360	*f*
PBTABQ-*co*-PBTHOBQ	0.110	300	*f*
PBTTBQ	0.060	390	*f*

[a] In DMF solution at 30 °C. [b] Onset of thermal decomposition in N_2 at 10 °C/min. [c] Measured in THF. [d] THF-soluble fraction. [e] Not measured. [f] Not detected up to 300 °C.

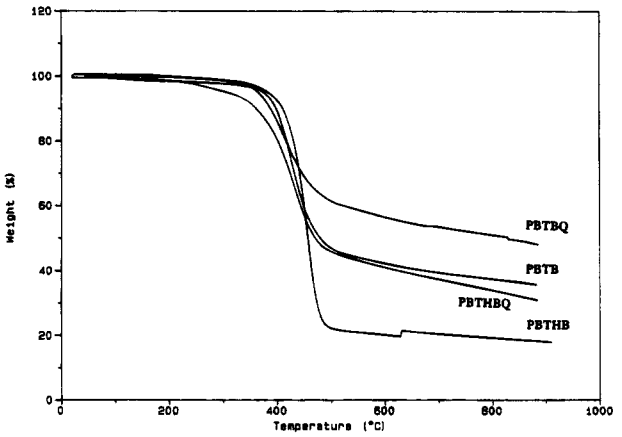

Figure 7. TGA curves of PBTB, PBTBQ, PBTHB, and PBTHBQ obtained in flowing N_2 at a heating rate of 10 °C/min.

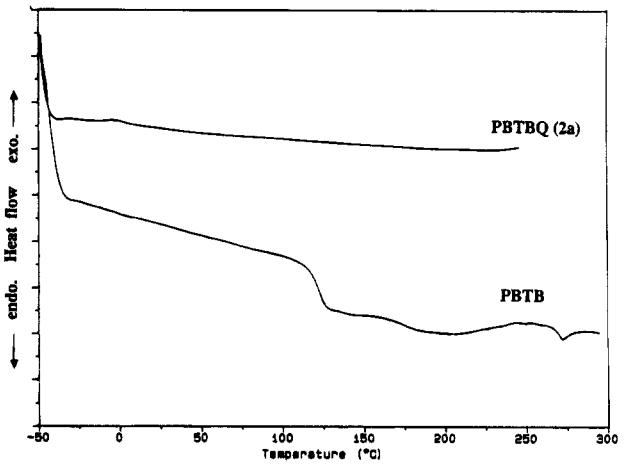

Figure 8. DSC curves of PBTB and PBTBQ obtained in flowing N_2 at a heating rate of 20 °C/min.

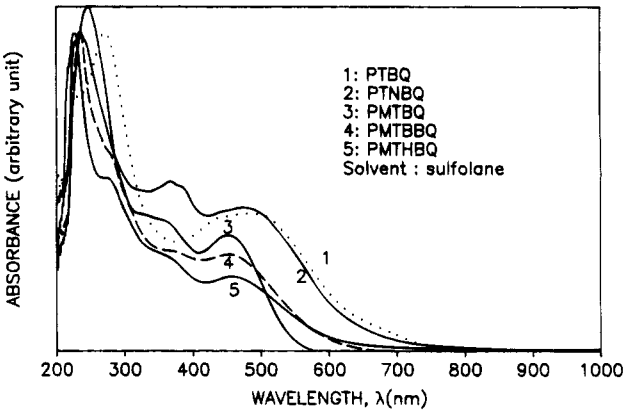

Figure 9. Optical absorption spectra of PTBQ (1), PTNBQ (2), PMTBQ (3), PMTBBQ (4), and PMTHBQ (5) in sulfolane.

nature of the polymers and the bulky side group at the methine carbon. PBTBQ, PBTNBQ, and PBTABQ-*co*-PBTHOBQ were only partially soluble in THF, DMF, or NMP although their precursors were very soluble in organic solvents. By substituting a long heptyloxy side chain on the phenyl ring, PBTHBQ was very soluble in THF, DMF, or CH_2Cl_2.

The intrinsic viscosities of the poly(heteroarylene methines) in DMF at 30 °C are collected in Table 4. All the dehydrogenated polymers have larger intrinsic viscosities than their corresponding precursor polymers.[32] For example, the $[\eta]$ values of PBTBQ and PBTNBQ are about twice those of their precursors PBTB and PBTNB. The observed increase in the intrinsic viscosity of the dehydrogenated polymers compared to the corresponding precursors is due to the greater stiffness of the polymer backbone of the conjugated polymers.

Thermal Properties. The thermal stability of the poly(heteroarylene methines) was investigated by thermogravimetric analysis (TGA). Figure 7 shows the TGA curves of PBTB, PBTHB, PBTBQ, and PBTHBQ obtained in a nitrogen atmosphere at a heating rate of 10 °C/min. PBTHBQ and PBTBQ are thermally stable with an onset of decomposition temperature (T_d) greater than 350 °C. The difference in the onset of thermal decomposition between PBTBQ and PBTHBQ and their precursors is insignificant. However, the weight residue at 800 °C was higher for PBTBQ and PBTHBQ than their precursors. The onset of thermal decomposition (T_d) of all the poly(heteroarylene methines), collected in Table 4, was between 300 and 390 °C.

Figure 8 shows the DSC curves of PBTB and PBTBQ at a heating rate of 20 °C/min under flowing nitrogen. The glass transition temperature (T_g) of PBTB is 122 °C. However, the conjugated polymer PBTBQ did not show a T_g up to 250 °C. This indicates that a large increase of the T_g has occurred after dehydrogenation reaction as might be expected. The glass transition temperatures of PBTHB, PBTHBQ1, and PBTHBQ2 were found to be 3, 25, and 33 °C, respectively, whereas the T_g of the 100% dehydrogenated polymer was not observable up to 300 °C. These results suggest that T_g increases with increasing degree of dehydrogenation. PMTBBQ with a T_g of 104 °C also shows an increase of T_g by about 36 °C compared to that of its precursor polymer, PMTBB. The T_g values of the dehydrogenated polymers are collected in Table 4. In general, the T_g values of the conjugated polymers are expected to be larger than those of their precursors because of the increased stiffness of the polymer backbone. Thus, the observed generally larger T_g values of the poly(heteroarylene methines) compared to their precursor poly(heteroarylene methylenes) confirm their stiffer chains and conjugated polymer chains.

Optical Absorption Spectra. Figure 9 shows the solution optical absorption spectra of poly(2,5-thienylene methines) PTBQ, PTNBQ, PMTBQ, PMTBBQ, and PMTHBQ in sulfolane. The colors of the polymer solutions were either orange or red. The spectra in Figure 9 show two major absorption bands. The band around 230 nm is assigned to the $\pi-\pi^*$ transition of

Table 5. Solution and Solid-State Optical Properties of Poly(heteroarylene methines)

polymer	λ_{max} (nm) ($\log \epsilon$ (M^{-1} cm^{-1})) (solution)	λ_{max} (nm) (film)	E_g (eV) (film)
P3HT	435 (3.95)[a]	506	1.92
PTBQ	471 (3.80)[b]	474	1.91
PTNBQ	485 (4.01)[b]	500	1.79
PMTBQ	452 (3.92)[b]	462	1.94
PMTBBQ	453 (3.92)[b]	463	1.94
PMTHBQ	456 (3.76)[b]	467	1.92
PBTBQ	605 (4.40)[c]	619	1.27
PBTNBQ	650 (4.08)[c]	675	1.45
PBTHBQ	582 (4.17)[a]	618	1.14
PBTABQ-*co*-PBTHOBQ	527 (4.30)[a]	527	1.64
PBTTBQ	631 (4.27)[a]	652	1.31

[a] THF. [b] Sulfolane. [c] NMP.

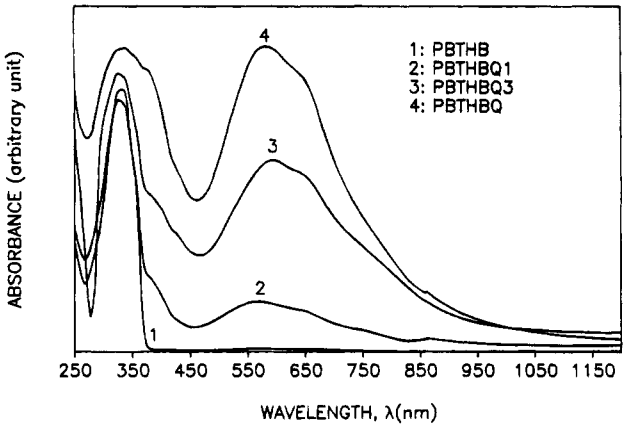

Figure 10. Optical absorption spectra of PBTHB (1), PBTHBQ1 (2), PBTHBQ3 (3), and PBTHBQ (4) in THF.

the aromatic thiophene ring since it corresponds to the same band in the precursors.[32] The band in the visible region which is in the range 452–485 nm is assigned to the π–π^* bandgap transition. The absorption spectra of thin films of PTBQ, PTNBQ, PMTBQ, PMTHBQ, and PMTHBQ have the lowest energy absorption maxima in the range of 462–503 nm. The corresponding absorption edges of the thin film spectra and hence optical bandgaps are in the range of 640–690 nm (1.79–1.94 eV). The bandgaps of these five polymers are slightly smaller than those of poly(3-alkylthiophenes) (~2.0 eV). The effect of the side group on the electronic structure is significant. PTBQ has a larger λ_{max} than PMTBQ, PMTBBQ, and PMTHBQ as shown in Table 5. This may be explained by the steric hindrance caused by the methyl group on the 3-position of the thiophene ring in PMTBQ, PMTBBQ, and PMTHBQ. The spectrum of thin films of PTNBQ shows a λ_{max} that is about 30 nm larger than that of PTBQ. Substitution of a nitro group at the phenyl ring extends π-electron delocalization, which may explain the higher λ_{max} of PTNBQ than that of PTBQ.

The poly(bithienylene methines), whose as-synthesized precursors were pure poly(bithienylene methylenes), provided an opportunity to monitor the evolution of their electronic structure with increasing degree of dehydrogenation. Figure 10 shows the solution optical absorption spectra of precursor PBTHB and the 20, 54, and 100% dehydrogenated derivatives in THF. The spectrum of precursor PBTHB has only one absorption band with a λ_{max} at about 326 nm, which is characteristic of the π–π^* absorption band of the aromatic bithiophene oligomer.[32] The spectrum of PBTHBQ1, which is 20% dehydrogenated, exhibits two absorption

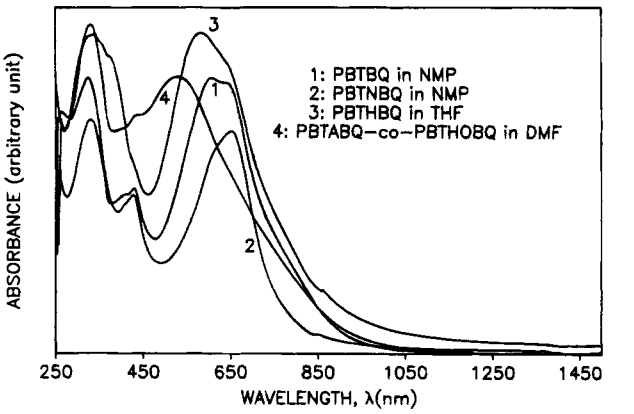

Figure 11. Solution electronic absorption spectra of PBTBQ (1, in NMP), PBTNBQ (2, in NMP), and PBTHBQ (3, in THF), and PBTABQ-*co*-PBTHOBQ (4, in DMF).

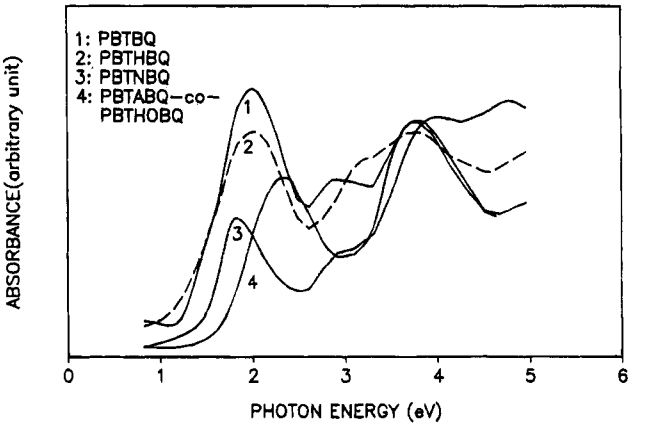

Figure 12. Optical absorption spectra of thin films of PBTBQ, PBTNBQ, PBTHBQ, and PBTABQ-*co*-PBTHOBQ on glass substrates.

bands, the strong 326 nm band and a weak band in the visible at 582 nm. The extinction coefficient of the visible absorption band $\lambda_{max} \approx 582$ nm in Figure 10 is seen to progressively increase with increasing degree of conversion of dehydrogenation reaction. The lowest energy absorption band of the solution spectrum of PBTHBQ in Figure 10 is assigned to the π–π^* bandgap transition. It was found that all the conjugated poly(heteroarylene methines) had lowest energy optical absorptions with significantly larger extinction coefficients than the corresponding nonconjugated precursor poly(heteroarylene methylenes). A collection of the λ_{max} and log ϵ of the solution optical spectra of the poly(heteroarylene methines) investigated is given in Table 5.

The solution optical absorption spectra of several poly(bithienylene methines) with different side groups at the methine carbon are shown in Figure 11. The absorption maxima of the spectra of these four polymers are in the range of 527–650 nm. The side group substituent at the methine carbon clearly has an effect on the electronic structure of these conjugated polymers.

The optical absorption spectra of thin films of the poly(heteroarylene methines) provided information about the optical bandgap (E_g), which is defined as the lowest energy band edge of the solid-state electronic spectra. Figure 12 shows the optical absorption spectra of the same conjugated polymers whose solution optical spectra were shown in Figure 11. The optical bandgaps of the polymers in Figure 12 are in the range 1.14–1.64 eV: PBTBQ (1.27 eV); PBTNBQ (1.45 eV); PBTHBQ

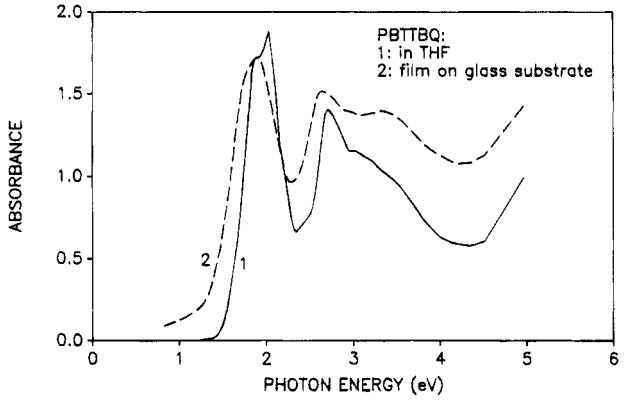

Figure 13. Optical absorption spectra of PBTTBQ: (1) in THF solution; (2) thin film on glass substrate.

(1.14 eV); and PBTABQ-*co*-PBTHOBQ (1.64 eV). The peak of the lowest energy absorption bands in these polymers was in the range of 1.8–2.4 eV (675–527 nm). Three of these polymers are indeed small-bandgap conjugated polymers with E_g values smaller than 1.5 eV. The variation of the bandgap among the polymers in Figure 12 is due solely to the variation of the side group at the methine carbon.

Figure 13 shows the solid-state and solution optical absorption spectra of PBTTBQ. In THF solution, the λ_{max} of the lowest energy absorption band of this polymer is 631 nm (1.97 eV) whereas it is red shifted to 652 nm (1.90 eV) in thin film. The optical bandgap of PBTTBQ obtained from the band edge of the thin film spectrum is 1.31 eV. Although PBTTBQ is not a degenerate ground state polymer with alternating quinoid terthienylene and aromatic terthienylene segments, the optical bandgap is remarkably smaller than that of polythiophene because of the incorporation of the quinoid terthienylene moiety in the polymer backbone.

An indication of the effect of the size of the quinoid thiophene oligomer on the E_g value can be obtained by comparing PTBQ, PBTBQ, and PBTTBQ (see Table 5). The bandgap decreases from 1.89 eV for PTBQ to 1.27 eV for PBTBQ and 1.31 eV for PBTTBQ. Since PBTTBQ is not strictly a degenerate ground state conjugated poly(heteroarylene methine) with alternating aromatic and quinoid segments of the same size, the apparent leveling off of E_g with heteroarylene size indicated in comparing PBTBQ with PBTTBQ is not an accurate conclusion. In fact, since the smallest observed E_g values (1.14 and 1.27 eV) were observed in members of poly(bithienylene methines), it is reasonable to expect that successful preparation of poly(terthienylene methines) will lead to observation of E_g values smaller than 1 eV. This expectation is consistent with the results of model compound studies.[31] Figure 14 is a schematic illustration of the effect of molecular structure on the optical bandgap (E_g) of polyheteroarylenes and poly(heteroarylene methines).

Electrochemical Properties. The electronic structure and properties of poly(heteroarylene methines) were further investigated by cyclic voltammetry. The electrochemical properties of poly(3-hexylthiophene) will be discussed first so that they can be to compared with those of poly(heteroarylene methines). Figure 15 shows the cyclic voltammogram (CV) of a thin film of poly(3-hexylthiophene) in the potential range of −2.5 to +1.35 V (vs SCE). The peak potentials (E_p) for electrochemical oxidation and reduction were observed at +0.88 and −2.10 V, respectively. The onset potentials (E_{on}) for oxidation and reduction were seen at +0.62 and −1.57 V, respectively, which correspond to an ionization potential (IP) of 5.02 eV and an electron affinity (EA) of 2.83 eV. The observed IP value of P3HT is very close to that of other poly(3-alkylthiophenes) (IP = 5.04–5.34 eV) reported in the literature.[39,46,47] The electrochemical bandgap of P3HT calculated from the difference between IP and EA is 2.19 eV, which is higher than the optical bandgap (1.92 eV) determined from the optical absorption spectra. In the electrochemical oxidation of P3HT, the anodic peak current was found to scale linearly with the sweep rate between 20 and 100 mV/s. This suggests that kinetic limitation on the electrochemical oxidation of P3HT is not significant.

The cyclic voltammograms of poly(heteroarylene methines) are exemplified by the cyclic voltammogram of PBTBQ. Figure 16 shows the overlay of the CVs of the electrochemical oxidation and reduction of PBTBQ in

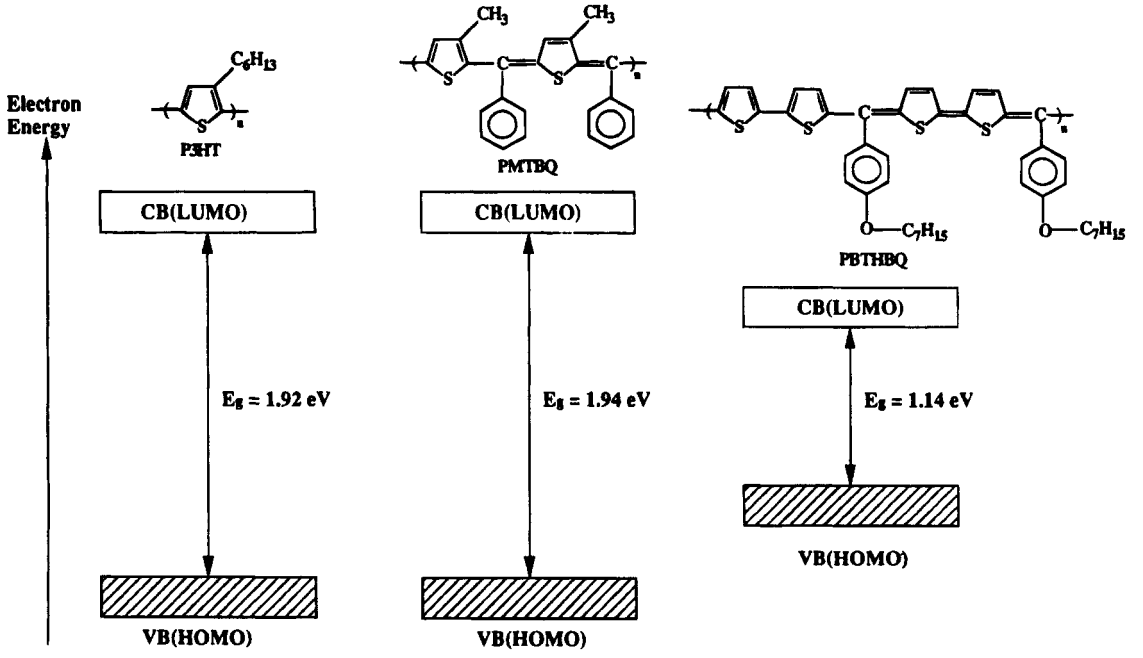

Figure 14. Schematic illustration of the effect of molecular structure on the optical bandgap of poly(heteroarylene methines).

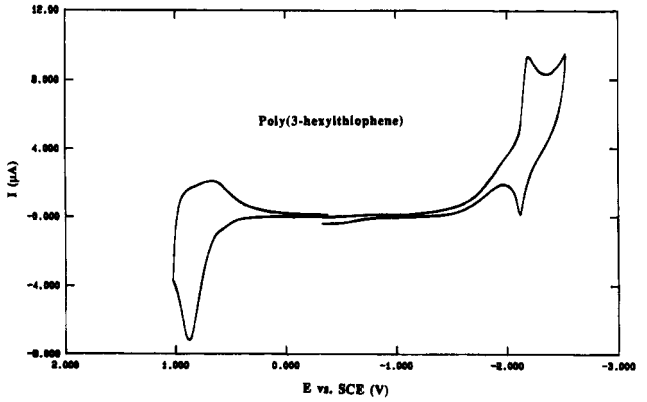

Figure 15. Cyclic voltammogram of the electrochemical oxidation and reduction of thin films of poly(3-hexylthiophene) in 0.1 M $TBAPF_6$ in acetonitrile at a sweep rate of 20 mV/s.

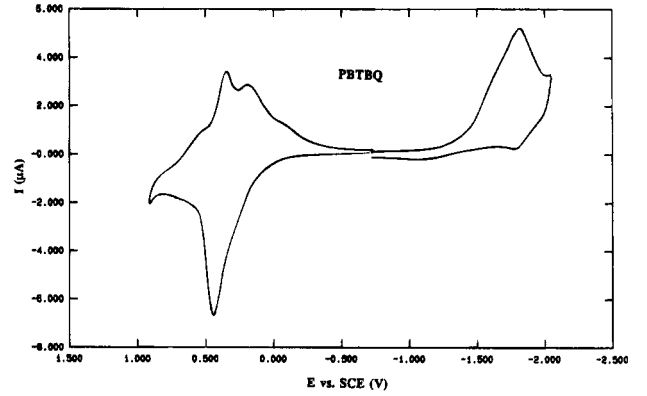

Figure 16. Cyclic voltammograms of the electrochemical oxidation and reduction of thin films of PBTBQ in 0.1 M $TBAPF_6$ in acetonitrile at a sweep rate of 20 mV/s.

the potential range of −2.2 to +0.9 V. The E_p values for oxidation and reduction were observed at +0.44 and −1.82 V, respectively, which are 0.44 and 0.28 V smaller and larger, respectively, than those of P3HT. The E_{on} for oxidation and reduction were observed at +0.06 and −1.26 V, respectively, which correspond to an IP of 4.46 eV and an EA of 3.14 eV. The electrochemical bandgap of PBTBQ determined from the difference between the IP and EA is 1.32 eV, which is 0.87 eV smaller than that of P3HT determined by the same method. This confirms the small-bandgap nature of PBTBQ previously indicated by its optical bandgap. At sweep rates between 40 and 100 mV/s, the anodic peak current of the CVs of PBTBQ was found to scale linearly with the square root of the sweep rate. This suggests that the electrochemical oxidation of PBTBQ exhibits more kinetic limitation than poly(3-hexylthiophene). This is

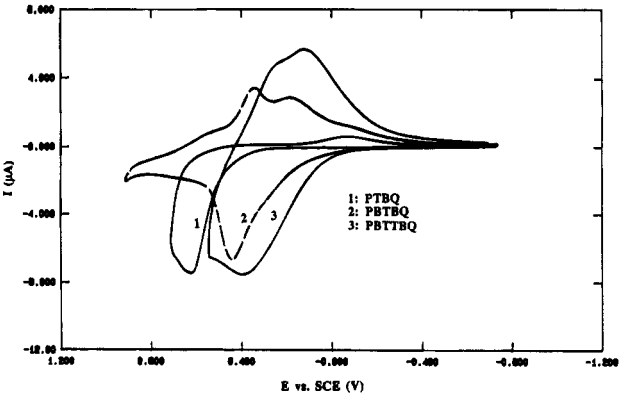

Figure 17. Cyclic voltammograms of the electrochemical oxidation of thin films of PTBQ, PBTBQ, and PBTTBQ in 0.1 M $TBAPF_6$ in acetonitrile at a sweep rate of 20 mV/s.

presumably due to poorer counterion diffusion in the polymer compared to P3HT.

The electrochemical properties of poly(heteroarylene methines) are collected in Table 6. The E_p values of the electrochemical oxidation of these polymers are in the range of 0.29−0.89 V, which are smaller than that of P3HT (0.88 V) except PMTHBQ (0.89 V). The E_{on} values of the electrochemical oxidation are in the range of 0.04−0.62 V, which correspond to IP values of 4.44−5.02 eV. These ionization potential values are smaller than or comparable with those of poly(3-alkylthiophenes) (5.04−5.34 eV),[39,46,47] polyacetylene (4.7 eV),[1a] poly(thiopheneylenevinylene) (4.76 eV),[48] and poly[(3-alkoxythiopheneylene)vinylene] (4.33−4.36 eV).[48] The peak and onset potentials of the electrochemical reduction of poly(heteroarylene methines) are in the range of −1.37 to −2.14 and −1.13 to −1.68 V, respectively. The corresponding EA values of these polymers are in the range of 2.72−3.27 eV, which are higher than that of P3HT except PTBQ and PMTBQ. The observed electrochemical bandgaps from the difference of IP and EA are in the range of 1.28−2.16 eV, which are in fair agreement with those determined from the optical absorption spectra except some of the poly(2,5-thienylene methines) **1**. Hence, the electrochemical results confirm the small bandgaps of PBTBQ, PBTNBQ, PBTHBQ, and PBTTBQ. The effects of the chemical structure on the electrochemical properties of the poly(heteroarylene methines) are also obvious from Table 6 as will be discussed in the following.

Effect of the Quinoid Thiophene Segment on the Electrochemical Properties. Figure 17 shows the cyclic voltammograms of thin films of PTBQ, PBTBQ, and PBTTBQ in the potential range of −0.8 to +1.0 V (vs SCE). The peak and onset potentials of the elec-

Table 6. Electrochemical Properties of Poly(heteroarylene methines) and Poly(3-hexylthiophene) (P3HT)

	oxidation (vs SCE)			reduction (vs SCE)			
polymer	E_p (V)	E_{on} (V)	IP (eV)	E_p (V)	E_{on} (V)	EA (eV)	E_g[a] (eV)
P3HT	0.88	0.62	5.02	−2.10	−1.57	2.83	2.19
PTBQ	0.62	0.39	4.79	−1.97	−1.60	2.80	1.99
PTNBQ	0.67	0.42	4.82	−1.37	−1.13	3.27	1.55
PMTBQ	0.83	0.48	4.88	−1.95	−1.68	2.72	2.16
PMTBBQ	0.73	0.54	4.94	−2.14	−1.40	3.00	1.94
PMTHBQ	0.89	0.62	5.02	*b*	−1.44	2.96	2.06
PBTBQ	0.44	0.06	4.46	−1.82	−1.26	3.14	1.32
PBTHBQ	0.29	0.08	4.48	−1.78	−1.20	3.20	1.28
PBTNBQ	0.54	0.16	4.56	−1.49	−1.24	3.16	1.40
PBTABQ-*co*-PBTHOBQ	0.83	0.38	4.78	*b*	−1.22	3.18	1.60
PBTTBQ	0.39	0.04	4.44	−1.67	−1.24	3.16	1.28

[a] Electrochemical bandgap E_g = IP − EA. [b] Not observed.

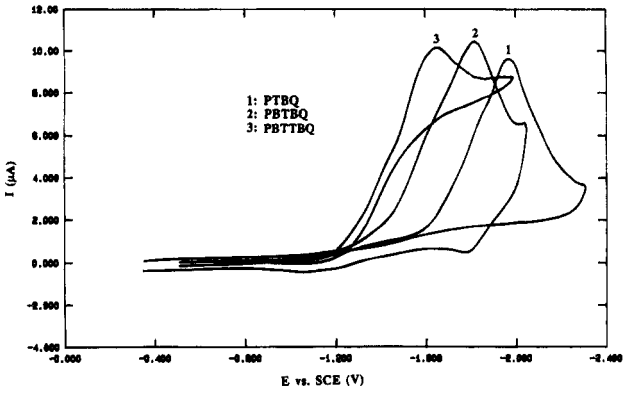

Figure 18. Cyclic voltammograms of the electrochemical reduction of thin films of PTBQ, PBTBQ, and PBTTBQ in 0.1 M $TBAPF_6$ in acetonitrile at a sweep rate of 20 mV/s.

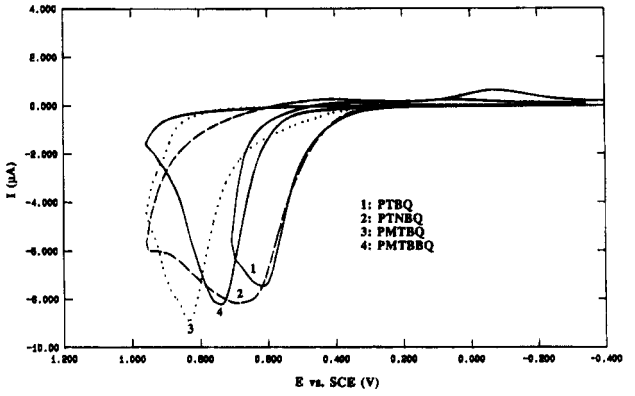

Figure 19. Cyclic voltammograms of the electrochemical oxidation of thin films of PTBQ, PTNBQ, PMTBQ, and PMTBBQ in 0.1 M $TBAPF_6$ in acetonitrile at a sweep rate of 20 mV/s.

trochemical oxidation decrease from 0.62 and 0.39 V for PTBQ to 0.44 and 0.06 V for PBTBQ and 0.39 to 0.04 V for PBTTBQ. The corresponding IP values determined from the onset potentials are 4.79 eV for PTBQ, 4.46 eV for PBTBQ, and 4.44 eV for PBTTBQ. The large decrease of the IP from PTBQ to PBTBQ indicates that the IP decreases with increasing size of the quinoid thiophene segment in the backbone. However, an insignificant change is observed between the ionization potential of PBTBQ and PBTTBQ. We have explained earlier that PBTTBQ is not strictly of the same structure as the other polymers, and hence an accurate comparison with it cannot be made. The size of the quinoid thiophene oligomer in the backbone also has a significant effect on the electrochemical reduction. Figure 18 shows the cyclic voltammograms of thin films of PTBQ, PBTBQ, and PBTTBQ in the potential range of −0.4 to −2.3 V (vs SCE). A gradual increase of the peak and onset potentials of the electrochemical reduction is observed from −1.97 and −1.60 V for PTBQ to −1.82 and −1.26 V for PBTBQ and −1.67 and −1.24 V for PBTTBQ, respectively. The corresponding EA increases from 2.80 eV for PTBQ to 3.14 eV for PBTBQ to 3.16 eV for PBTTBQ. Again, the large increase of the EA between PTBQ and PBTBQ is observed but it remains constant with insignificant change between PBTBQ and PBTTBQ.

Effect of the Side Group on the Electrochemical Properties. Figure 19 shows the cyclic voltammograms of PTBQ, PTNBQ, PMTBQ, and PMTBBQ in the potential range of −0.4 to 1.0 V. The E_p values of electrochemical oxidation are 0.62 V for PTBQ, 0.67 V for PTNBQ, 0.83 V for PMTBQ, and 0.73 V for PMTBBQ. PTNBQ has a slightly larger E_p value than PTBQ. This is as expected because the strong electron-withdrawing nitro group decreases the electron density in the backbone and thus is more difficult to be oxidized. For example, substitution of the nitro group on the 3-position of the thiophene ring results in an increase of 0.63 V on the E_p value.[49] Substitution of the weakly electron-donating methyl group on the 3-position of the thiophene ring may decrease the peak potential because it increases the electron density in the polymer backbone. However, PMTBQ shows an E_p value about 0.21 V larger than PTBQ. This may be explained by the steric hindrance caused by the methyl group and results in a decrease of π-electron delocalization on the polymer backbone. Such a steric effect can also be used to explain the larger peak potentials of the electrochemical oxidation of PMTBBQ and PMTHBQ than that of PTBQ despite their electron-donating side groups. This result is consistent with the previous comparison of the optical absorption spectra of PTBQ, PMTBQ, PMTBBQ, and PMTHBQ. The effect of the electron-donating alkoxy side group on the electrochemical oxidation can be further investigated from the comparison of the CVs and electrochemical properties of PBTBQ and PBTHBQ. The peak potential of the electrochemical oxidation of PBTHBQ is 0.15 V smaller than that of PBTHBQ (Table 6). However, the onset potential does not show a significant difference between these two polymers.

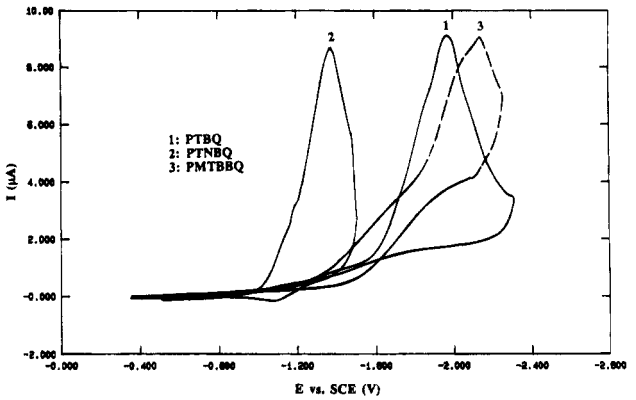

Figure 20. Cyclic voltammograms of the electrochemical reduction of thin films of PTBQ, PTNBQ, and PMTBBQ in 0.1 M $TBAPF_6$ in acetonitrile at a sweep rate of 20 mV/s.

Figure 20 shows the cyclic voltammograms of electrochemical reduction of PTBQ, PTNBQ, and PMTBBQ in the potential range of −0.4 to −2.4 V. The E_p value for the reduction was observed at −1.97 V for PTBQ, −1.37 V for PTNBQ, and −2.14 V for PMTBBQ. As discussed above, the nitro group reduces the electron density of the polymer backbone and hence is expected to be more easily reduced. On the other hand, the electron-donating group increases the electron density of the backbone and thus is expected to be more difficult to reduce. This explains the higher reduction peak potential of PTNBQ than PTBQ and the smaller reduction peak potential of PMTBBQ than PTBQ.

Electrical Conductivity and Doping Study. Electrical conductivity of films of the pristine (undoped) poly(heteroarylene methines) exemplified by PBTBQ (E_g = 1.27 eV), PBTNBQ (E_g = 1.45 eV), and PBTHBQ (E_g = 1.14 eV), measured by the four-point probe technique at room temperature, was found to be less than 10^{-7} S/cm. Clearly, such a low intrinsic conductivity does not qualify the present polymers to be considered good intrinsic conductors in spite of their small intrinsic bandgaps. However, the present results are not un-

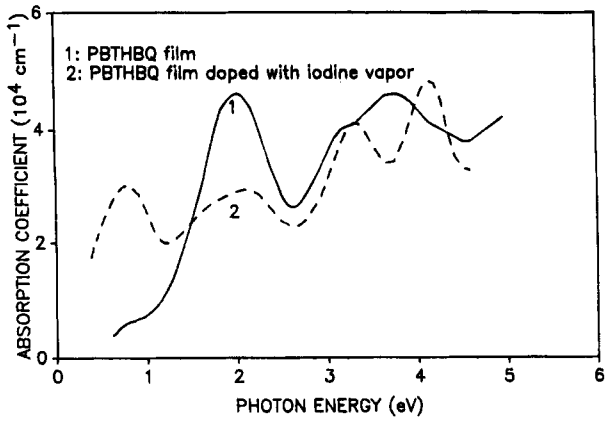

Figure 21. Optical absorption spectra of thin films of PBTHBQ on glass substrates: (1) undoped film; (2) iodine-doped film.

usual since the E_g value is not the only factor that determines the conductivity of a material. Among inorganic semiconductors, for example, silicon ($E_g = 1.11$ eV)[50] with a bandgap comparable with PBTHBQ ($E_g = 1.14$ eV) has an intrinsic conductivity[50] of only 5×10^{-6} S/cm. Intrinsic conductivities vary widely among inorganic semiconductors[50] with $E_g < 1.5$ eV; for example, GaAs ($E_g = 1.4$ eV, $\sigma = 10^{-8}$ S/cm); germanium ($E_g = 0.66$ eV, $\sigma = 2 \times 10^{-2}$ S/cm); InP ($E_g = 1.3$ eV, $\sigma = 5$ S/cm); and InAs ($E_g = 0.36$ eV, $\sigma = 10^2$ S/cm). The electron mobilities (μ_e) in these cited inorganic semiconductors are quite high values[50] in the range of 1.9×10^3 to 2.26×10^4 cm^2/V-s. The electron or hole mobilities in the poly(heteroarylene methines), as in other conjugated polymers, are expected to be several orders of magnitude smaller. Specifically, the low molecular weight,[32] low charge carrier mobilities, low carrier concentrations, and bulky side groups may explain the small intrinsic conductivity of the poly(heteroarylene methines). From theoretical calculation, the bandwidth of poly(*p*-phenylene methine)[8b] and poly(pyrrolylene methine)[14] were estimated to be 0.44 and 1.97 eV, respectively, which were smaller than their parent poly(*p*-phenylene) (3.5 eV) and poly(pyrrole) (2.44 eV). This suggests that poly(arylene methines) have smaller bandwidths than their parent conjugated polymers. Hence, it is also possible that the bandwidth of poly(thienylene methine) is smaller than that of the parent polythiophene. Small bandwidth reduces charge carrier mobility and results in poor conductivity.

Thin films of PBTBQ, PBTNBQ, and PBTHBQ, when doped with iodine vapor, have room temperature conductivities of 6×10^{-3}, 2.2×10^{-2}, and 1.6×10^{-1} S/cm, respectively. This represents about a 4–6 order of magnitude increase above the intrinsic conductivity. The conductivity of these three iodine-doped polymers was stable in air for a few days. The estimated level of doping of these polymers was 28–33% I_3^- by weight uptake. The conductivity of iodine-doped poly(bithienylene methines) is smaller than that of similarly iodine-doped poly(3-alkylthiophenes), which is in the range of 3–27 S/cm for a 9–17% I_3^- level of doping.[51,52] The differences in molecular weight and bandwidth (charge carrier mobility) of poly(3-alkylthiophenes) and poly(thienylene methines) appear to be the origin of the difference in conductivity of the doped polymers.

The effect of iodine doping on the optical absorption spectrum of PBTHBQ is shown in Figure 21. The optical absorption spectrum of iodine-doped PBTHBQ thin film is characterized by a large decrease of the oscillator strength of the π–π^* absorption maximum at 2 eV (618 nm) and the appearance of a new absorption band at 0.78 eV (1596 nm). ESR study of the doped PBTBQ and PBTHBQ showed an ESR signal with a spin concentration of 1.63×10^{19} spin/g ($\Delta H_{pp} = 6.5$ G, $g = 2.005279$) and 1.18×10^{19} spin/g ($\Delta H_{pp} = 6.5$ G, $g = 2.005954$), respectively. The observed spin concentration in the doped polymers is 4 and 5 times larger than the undoped PBTBQ and PBTHBQ. The large increase of spin concentration after doping of PBTHBQ may indicate the formation of polarons. However, the observed single sub-bandgap absorption band in the doped polymer is not sufficient to assign the origin of the charged species in the doped polymers.

Conclusions

In this paper, we have reported the successful synthesis and a detailed characterization of many soluble conjugated poly(heteroarylene methines) which contain alternating aromatic and quinoid thiophene oligomers. It was shown from optical absorption spectra and electrochemical experiments that some of the conjugated poly(heteroarylene methines) have an *intrinsic* bandgap (E_g) as small as 1.14 eV. The intrinsic conductivity of the small bandgap polymers was less than 10^{-7} S/cm. However, iodine-doped films of some of the polymers have conductivities of about 10^{-3}–10^{-1} S/cm. These results suggest that achieving small bandgaps (1 eV or even less) in polymers is not sufficient to significantly increase the intrinsic conductivity in accord with similar results in inorganic semiconductors. Such small-bandgap conducting polymers are nevertheless interesting electronic and optoelectronic materials that may find other applications.

These results also confirm that conjugated poly(heteroarylene methines) are small-bandgap conducting polymers that can be prepared by oxidative dehydrogenation of precursor polymers.[3] The structure of the poly(heteroarylene methines), particularly the size of the thiophene oligomers incorporated in the backbone and the nature of the side group at the methine carbon, were shown to significantly modify the optical, redox, T_g, and other physical properties.

Acknowledgment. This research was supported by the NSF Center for Photoinduced Charge Transfer (Grant CHE-912-0001), the Amoco Foundation, and an Elon Huntington Hooker Fellowship to W.-C.C.

References and Notes

(1) (a) Skotheim, T. A., Ed. *Handbook of Conducting Polymers*; Marcel Dekker: New York, 1986. (b) Bredas, J. L.; Chance, R. R., Eds. *Conjugated Polymeric Materials: Opportunities in Electronics, Optoelectronics, and Molecular Electronics*; Kluwer Academic Publishers: Dordrecht, Holland, 1990. (c) Bredas, J. L.; Sibley, R., Eds. *Conjugated Polymers: The Novel Science and Technology of Highly Conducting and Nonlinear Optically Active Materials*; Kluwer Academic Publishers: Dordrecht, Holland, 1991. (d) Kiess, H. G., Ed. *Conjugated Conducting Polymers*; Springer Series in Solid State Science; Springer-Verlag: Berlin, Heidelberg, 1992; Vol. 102.

(2) Basescu, N.; Liu, Z.-X.; Moses, D.; Heeger, A. J.; Naarmann, H.; Theophilou, N. *Nature* **1987**, *327*, 403–405.

(3) (a) Jenekhe, S. A. *Nature* **1986**, *322*, 345–347. (b) Jenekhe, S. A. *Macromolecules* **1986**, *19*, 2663–2664.

(4) (a) Bredas, J. L.; Baughamn, R. H. *J. Polym. Sci., Polym. Lett. Ed.* **1983**, *21*, 475–479. (b) Bredas, J. L.; Themans, B.; Andre, J. L. *J. Chem. Phys.* **1983**, *78*, 6137–6148.

(5) (a) Bredas, J. L. *Mol. Cryst. Liq. Cryst.* **1985**, *118*, 49–56. (b) Bredas, J. L.; Heeger, A. J.; Wudl, F. *J. Chem. Phys.* **1986**, *85*, 4673–4678.
(6) Hoogmartens, I.; Adriaensens, P.; Vanderzande, D.; Gelan, J.; Quattrocchi, C.; Lazzaroni, R.; Bredas, J. L. *Macromolecules* **1992**, *25*, 7347–7356.
(7) (a) Hong, S. Y.; Marynick, D. S. *J. Chem. Phys.* **1992**, *96*, 5497–5504. (b) Hong, S. Y.; Marynick, D. S. *Macromolecules* **1992**, *25*, 4652–4657.
(8) (a) Bredas, J. L.; Boudreaux, D. S.; Chance, R. R.; Sibley, R. *Mol. Cryst. Liq. Cryst.* **1985**, *118*, 323–326. (b) Boudreaux, D. S.; Chance, R. R.; Elsenbaumer, R. L.; Frommer, J. E.; Bredas, J. L.; Sibley, R. *Phys. Rev. B* **1985**, *31*, 652–655.
(9) (a) Lee, Y. S.; Kertesz, M. *J. Chem. Phys.* **1988**, *88*, 2609–2617. (b) Kertesz, M.; Lee, Y. S. *J. Phys. Chem.* **1987**, *91*, 2690–2692. (c) Lee, Y. S.; Kertesz, M.; Elsenbaumer, R. L. *Chem. Mater.* **1990**, *2*, 526–530.
(10) Toussaint, J. M.; Themans, B.; Andre, J. M.; Bredas, J. L. *Synth. Met.* **1989**, *28*, C205–C210.
(11) Pranata, J.; Marudarajan, V. S.; Dougherty, D. A. *J. Am. Chem. Soc.* **1989**, *111*, 2026–2030.
(12) (a) Tanaka, K.; Wang, S.; Yamabe, T. *Synth. Met.* **1989**, *30*, 57–65. (b) Tanaka, K.; Wang, S.; Yamabe, T. *Synth. Met.* **1990**, *39*, 225–231.
(13) Otto, P.; Ladik, J. *Synth. Met.* **1990**, *36*, 327–335.
(14) Toussaint, J. M.; Bredas, J. L. *J. Chem. Phys.* **1991**, *94*, 8122–8128.
(15) Cui, C. X.; Kertesz, M. *J. Am. Chem. Soc.* **1991**, *113*, 4404–4409.
(16) Toussaint, J. M.; Bredas, J. L. *Synth. Met.* **1992**, *46*, 325–335.
(17) Agrawal, A. K.; Jenekhe, S. A., unpublished results.
(18) (a) Murakami, M.; Yoshimura, S. *Mol. Cryst. Liq. Cryst.* **1985**, *118*, 95–102. (b) Iqbal, Z.; Ivory, D. M.; Marti, J.; Bredas, J. L. *Mol. Cryst. Liq. Cryst.* **1985**, *118*, 103–110.
(19) (a) Kobayashi, M.; Colaneri, N.; Boysel, M.; Wudl, F.; Heeger, A. J. *J. Chem. Phys.* **1985**, *82*, 5717–5723. (b) Ikenoue, Y.; Wudl, F.; Heeger, A. J. *Synth. Met.* **1991**, *40*, 1–12.
(20) Chandrasekhar, P.; Masulaitis, A. M.; Gumbs, R. W. *Synth. Met.* **1990**, *36*, 303–326.
(21) (a) Patil, A. O.; Wudl, F. *Polym. Prepr. (Am. Chem. Soc., Div. Polym. Chem.)* **1987**, *28* (2), 341–342. (b) Patil, A. O.; Wudl, F. *Macromolecules* **1988**, *21*, 540–542.
(22) (a) Moreno, V. P. A.; Rodero, A.; Fernandez, J. E. *J. Org. Chem.* **1982**, *47*, 3986–3987. (b) Fernandez, J. E.; Al-Jumah, K. *Macromolecules* **1984**, *17*, 2935–2937. (c) Al-Jumah, K.; Fernandez, J. E. *Macromolecules* **1987**, *20*, 1177–1180.
(23) (a) Braunling, H.; Jira, R. *Synth. Met.* **1987**, *20*, 375–378. (b) Jira, R.; Braunling, H. *Synth. Met.* **1987**, *17*, 691–696. (c) Becker, R.; Blochl, G.; Braunling, H. In ref 1b, pp 133–139. (d) Wehrle, B.; Limbach, H.-H.; Braunling, H. *Synth. Met.* **1991**, *39*, 319–325. (e) Braunling, H.; Blochl, G.; Becker, R. *Synth. Met.* **1991**, *41–43*, 487–491. (f) Braunling, H.; Becker, R.; Blochl, G. *Synth. Met.* **1991**, *41–43*, 1539–1547.
(24) (a) Hanack, M.; Dewald, G. *Synth. Met.* **1989**, *39*, 409–414. (b) Hanack, M.; Hieber, G.; Dewald, G.; Ritter, H.; Rohrig, U. *Polym. Mater. Sci. Eng. (Am. Chem. Soc., Div. Polym. Mater. Sci. Eng.)* **1991**, *64*, 330–331. (c) Hanack, M.; Hieber, G.; Dewald, G.; Ritter, H. *Synth. Met.* **1991**, *41–43*, 507–511. (d) Hieber, G.; Hanack, M.; Wurst, K.; Strahle, J. *Chem. Ber.* **1991**, *124*, 1597–1605.
(25) Talianni, C.; Zamboni, R.; Ruani, G.; Ostoia, P.; Bolognesi, A.; Catellani, M.; Destri, S.; Porzio, W. In *Nonlinear Optical Effects in Organic Polymers*; Messier, J., Kajzar, F., Prasad, P., Ulrich, D. R., Eds.; Kluwer Academic Publishers: Dordrecht, Holland, 1989; pp 159–172.
(26) (a) Lambert, T. L.; Ferraris, J. P. *J. Chem. Soc., Chem. Commun.* **1991**, 752–754. (b) Ferraris, J. P.; Lambert, T. L. *J. Chem. Soc., Chem. Commun.* **1991**, 1268–1270.
(27) (a) Kowalik, J.; Nguyen, H. T.; Tolbert, L. M. *Synth. Met.* **1991**, *41–43*, 435–438. (b) Kowalik, J.; Tolbert, L. M. *Polym. Mater. Sci. Eng.* **1991**, *64*, 214–215.
(28) Havinga, E. E.; ten Hoeve, W.; Wynberg, H. *Polym. Bull.* **1992**, *29*, 119–126.
(29) Walker, D.; Hiebert, J. D. *Chem. Rev.* **1967**, *67*, 153–195.
(30) Becker, H.-D.; Turner, A. B. In *The Chemistry of the Quinonoid Compounds*; Patai, S., Rappoport, Z., Eds.; John Wiley & Sons: New York, 1988; Vol. 2, pp 1351–1384.
(31) Chen, W. C.; Jenekhe, S. A., in preparation.
(32) Chen, W. C.; Jenekhe, S. A. *Macromolecules* **1995**, *28*, 454.
(33) (a) Jenekhe, S. A.; Lo, S. K.; Flom, S. R. *Appl. Phys. Lett.* **1989**, *54*, 2524–2526. (b) Jenekhe, S. A.; Chen, W. C.; Flom, S. R.; Lo, S. K. *Appl. Phys. Lett.* **1990**, *57*, 126–128. (c) Meth, J. S.; Vanherzeele, H.; Chen, W. C.; Jenekhe, S. A. *Synth. Met.* **1992**, *49–50*, 59–69.
(34) Jenekhe, S. A. *Macromolecules* **1990**, *23*, 2848–2854.
(35) *CRC Handbook of Chemistry and Physics*, 68th ed.; CRC Press: Boca Raton, FL, 1987; pp D151–D158.
(36) Chance, R. R.; Boudreaux, D. S.; Bredas, J. L.; Sibley, R. *ACS Symp. Ser.* **1984**, *No. 242*, 433–446.
(37) Miller, L. L.; Nordbolm, G. D.; Mayeda, E. A. *J. Org. Chem.* **1972**, *37*, 916–918.
(38) Sato, N.; Seki, K.; Inokuchi, H. *J. Chem. Soc., Faraday Trans.* **1981**, *77*, 1621–1633.
(39) Leclerc, M.; Martinez, F.; Wegner, G. *Makromol. Chem.* **1989**, *190*, 3105–3116.
(40) Daoust, G.; Leclerc, M. *Macromolecules* **1991**, *24*, 455–459.
(41) Reid, D. H.; Fraser, M.; Molloy, B. B.; Payne, H. A.; Sutherland, R. G. *Tetrahedron Lett.* **1961**, 530–535.
(42) Macdonagh, A. F.; Plama, L. A. *Biochem. J.* **1980**, *189*, 193–208.
(43) Chen, W. C.; Jenekhe, S. A. *Macromolecules* **1992**, *25*, 5919–5926.
(44) (a) In ref 1a, pp 1099–1125. (b) Scott, J. C.; Pfluger, P.; Krounbi, M. T.; Street, G. B. *Phys. Rev. B* **1983**, *28*, 2140–2145. (c) Gourley, K. D.; Lillya, C. P.; Reynolds, J. R.; Chien, J. C. W. *Macromolecules* **1984**, *17*, 1025–1033.
(45) Furukawa, Y.; Akimoto, M.; Harada, I. *Synth. Met.* **1987**, *18*, 151–156.
(46) Roncali, J.; Garreau, R.; Yassar, A.; Marque, P.; Garnier, F.; Lemaire, M. *J. Phys. Chem.* **1987**, *97*, 6706–6714.
(47) Yassar, A.; Roncali, J.; Garnier, F. *Macromolecules* **1989**, *22*, 804–809.
(48) Eckhardt, H.; Shacklette, L. W.; Jen, K. Y.; Elsenbaumer, R. L. *J. Chem. Phys.* **1989**, *91*, 1303–1315.
(49) Waltman, R. J.; Diaz, A. F.; Bargon, J. *J. Electrochem. Soc.* **1984**, *131*, 1452–1456.
(50) (a) Kittel, C. *Introduction to Solid State Physics*; Wiley: New York, 1986; Chapter 8. (b) Van Vlack, L. H. *Elements of Materials Science and Engineering*, 6th ed.; Addison-Wesley: Reading, MA, 1989; p 413.
(51) Jen, K.-Y.; Miller, G. G.; Elsenbaumer, R. L. *J. Chem. Soc., Chem. Commun.* **1986**, 1346–1347.
(52) Hotta, S.; Soga, M.; Sonoda, N. *Synth. Met.* **1988**, *26*, 267–269.

MA9410680